"POCK MARKS" IN NEARSHORE SANDS: OBSERVATIONS DURING SANDYDUCK97

Rachel H. Speller

Submitted in partial fulfillment of the

Requirements for the degree of Bachelor of Science, Honours

Department of Earth Sciences

Dalhousie University, Halifax, Nova Scotia

March, 2000

Dalhousie University

Department of Earth Sciences
Halifax, Nova Scotia
Canada B3H 3J5
(902) 494-2358
FAX (902) 494-6889

DATE April 17, 2000

AUTHOR Rachel H Speltker

TITLE "Pock Marks" in Nearshore Sands: Observations During SandyDuck97

Degree BSc Convocation May 23 Year 2000

Permission is herewith granted to Dalhousie University to circulate and to have copied for non-commercial purposes, at its discretion, the above title upon the request of individuals or institutions.

ABSTRACT

Previous bedform research has described different ripple types forming in varying hydrodynamic conditions and used ripple geometry within sedimentary rocks to infer the paleoenvironmental conditions during the ripple formation. During the 1997 SandyDuck97 nearshore dynamics experiment at the U. S. Army Engineers Waterways Experiment station's field research facility at Duck, North Carolina, rotary fan beam sonar was used to collect images of the characteristics of the sea floor. In these images, curious depressions were observed to form in the seabed during storm growth and decay. These "pock marks" are circular depressions with an average diameter of 15-20cm and a depth of 3cm. By studying the spatial and temporal characteristics of pock marks such as size, shape, number per unit area, and group lifetime, and relating these to flow energy it was determined that these features form in a wave orbital velocity range of 50-115cm/s and during the growth and decay phase of individual storm events. Also studied is the mode of formation of the pock marks (i.e. shell/pebble nucleus) and their role as a precursor to lunate megaripple genesis.

ACKNOWLEGEMENTS

First and foremost I wish to thank those most directly involved in the project: Dr. Alex Hay who not only provided me with the opportunity to conduct research in the Oceanography Department, but also with his friendly encouragement, patience, and support; Dr. Martin Gibling and Dr. Marcos Zentilli for their insights, suggestions, and motivational words; and finally to Todd Mudge for his invaluable technical expertise and Dan Petrie who wrote the Matlab codes, without which I could never have begun 8 months ago.

More generally, I wish to extend my thanks to the faculty and students who have supported and inspired me throughout my five years at Dalhousie. I thank you for making my undergraduate career both enriching and enjoyable.

Finally, I wish to thank my family and loved ones for their constant support and encouragement, and for instilling in me the values and work ethic required to survive a degree and to face the challenges ahead.

TABLE OF CONTENTS

LIST OF TABLES

Number *Page*

LIST OF FIGURES

Number *Page*

Chapter 1: INTRODUCTION

In 1997, an international group of scientists assembled at the U. S. Army Engineers Waterways Experiment station's field research facility in North Carolina for the SandyDuck97 experiment, a multipurpose experiment to study coastal sediment transport, morphology of the seafloor, and wave motion in a nearshore environment. A group from Canada conducted an investigation of nearshore sediment dynamics. One component of this investigation was carried out by Dalhousie's Ocean Acoustic Laboratory using rotary fan and pencil beam sonar to collect acoustic data of the ocean bottom. During the course of the experiment, curious depressions in the seafloor with horizontal scales of about 10-30cm were observed, and these occasionally developed into lunate megaripples. These features, which are referred to in this thesis as "pock marks", have not been previously reported in the literature and, in part because of their possible role in megaripple genesis, may be quite important. Due to the significant bottom roughness of megaripples, understanding how and why these features form is important for sediment transport prediction in the nearshore environment. Preliminary analysis of the data indicated a tendency for pock marks to occur in a narrow range of wave orbital velocity amplitudes. This suggested that their occurrence might be predictable if the wave and current conditions are known.

The initial goal of this thesis was to carry out a comprehensive examination of the SandyDuck97 data in order to determine all instances of pock mark occurrence. A database was then created of those occurrences, and pock mark geometric properties and migration. The objective is to quantitatively determine the relationships between pock

mark formation and the fluid forcing parameters, and to discover under what circumstances these features transform into lunate megaripples.

1.1 Previous Work

Tracing research studies of nearshore dynamics through time, there is a progression not only in the classification of bedforms but also in the understanding of their relationship to hydrodynamics. This has led to the concept of predicting the types of bedforms found in nearshore environments through the hydrodynamics of the area and finally relating this knowledge to understanding the conditions of paleoenvironments and to determining sediment transport mechanisms.

Bagnold (1946) performed an experiment in which the sand was on a tray that could oscillate through a circular arc in a tank containing still water. From this he described two ripple types: rolling grain ripples and vortex ripples. Rolling grain ripples form when minimum water motion causes grains to begin to roll. As water motion increases grains become organized into parallel transverse zones, then small wavy ridges. The ripples show no grain movement in the trough and are stable from the speed at the time of first motion to twice that speed. Vortex ripples begin from a surface irregularity and form when the water speed becomes high enough to cause flow separation from the bed at the ripple crest and the creation of a lee vortex.

Dingler and Inman (1976) experimented in La Jolla, California using high-resolution sonar. From a plot of ripple steepness η/λ (which Nelson (1981) calculated using shear stress Φ' and the angle of repose β) versus the waveform of Shields relative stress criterion θ, they classified ripples into vortex, relict, and transition types. Dingler

and Inman (1976) also calculated the limits of each ripple regime; vortex ripples have a steepness of 0.15 and transition ripples have a steepness of < 0.15.

Clifton (1976) created a conceptual model based on maximum bottom orbital velocity, velocity asymmetry, median grain size, and wave period. He described 3 ripple types formed by symmetrical waves: 1) orbital ripples form in short period waves, have an d_0/D (diameter of orbital motion/median grain diameter) less than 2000, and a ripple spacing dependent on grain diameter and related to the length of the orbital diameter, 2) suborbital ripples form in longer period waves, have a d_0/D of 2000 to 5000, and a ripple

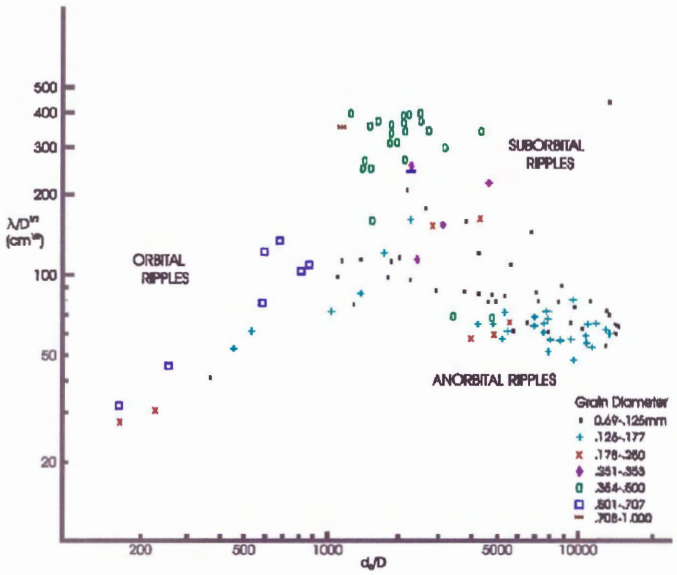

Figure 1.1 Graph illustrating d_0/D ranges of orbital, sub-orbital and anorbital ripples. Modified from Clifton, 1976.

spacing dependent on grain diameter and inversely related to orbital diameter, and 3) anorbital ripples form when wave periods are dependent on grain diameter, have a d_0/D greater than 5000, and a ripple spacing independent of orbital diameter and dependent on grain diameter (Fig.1.1). Clifton (1976) also found that, moving from deep to shallow water, bedforms change with increasing velocity and velocity asymmetry from long-

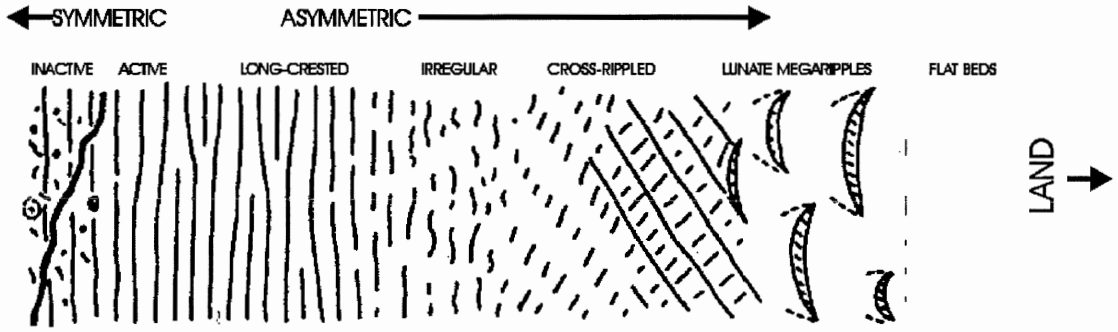

Figure 1.2 Illustration of the sequence of bedforms as you move from deep to shallow water. Modified from Clifton, 1976.

crested ripples, to irregular ripples, to cross ripples, to lunate megaripples, and finally to flat bed (Fig.1.2). He calculated that the transition from symmetric ripples to asymmetric ripples occurs within a velocity asymmetry range of 1-5cm/sec. Hay and Wilson (1994) used rotating fan-beam sidescan sonar in order to study large bedforms (i.e. lunate megaripples) in more than one dimension, and with a range of 5 m and a spatial resolution of 1 cm. They noticed a progression through time during a storm of ripple types from irregular ripples, to oblique cross ripples with patchy shore-parallel ripples and few megaripples, to long-crested, shore-parallel ripples with some megaripples, to flat bed. Hay and Wilson (1994) described shore-parallel ripples as the transition between suborbital and anorbital ripples. This indicates that Clifton's (1976) progression of bedforms from deep to shallow water occurs in one location on the seafloor during the progression of a storm event.

Hunter et al. (1979) studied sedimentary structures in the barred nearshore and divided the region into six facies (Fig.1.3). The inner offshore facies contains asymmetric, small scale, short-crested sand ripples normal to the storm surge. The bar facies is the region at the limit of megaripple occurrence under normal wave conditions where the

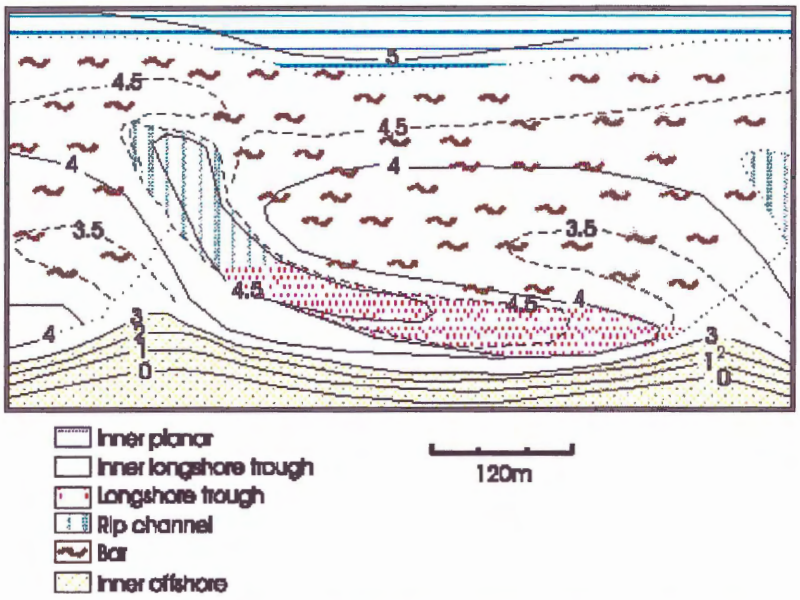

Figure 1.3 Six facies seen in the barred nearshore. Modified from Hunter et al., 1979.

megaripples migrate in the direction of wave propagation. Longshore trough facies contain transverse beds in the longshore direction and mainly linguoid megaripples and irregular ripples. The rip channel facies has megaripples in a seaward direction. In the inner longshore trough is a beach toe with seaward facing lunate megaripples and seaward, long-crested ripples. Finally, the inner planar facies constitutes the swash zone of the beach and contains parallel laminations. Hunter et al. (1979) described a vertical sequence containing all of these features.

Clifton et al. (1971) studied sedimentary structures in the non-barred nearshore and described five different facies (Fig.1.4). The inner planar facies is again in the swash zone and has a planar surface. The inner rough facies is between the surf and the swash zones and contains steep sided, symmetric ripples whose crests are parallel to the beach. The outer planar facies is mainly flat with few small, long-crested sand ripples. In the outer rough facies are landward facing lunate megaripples with variable size and spacing.

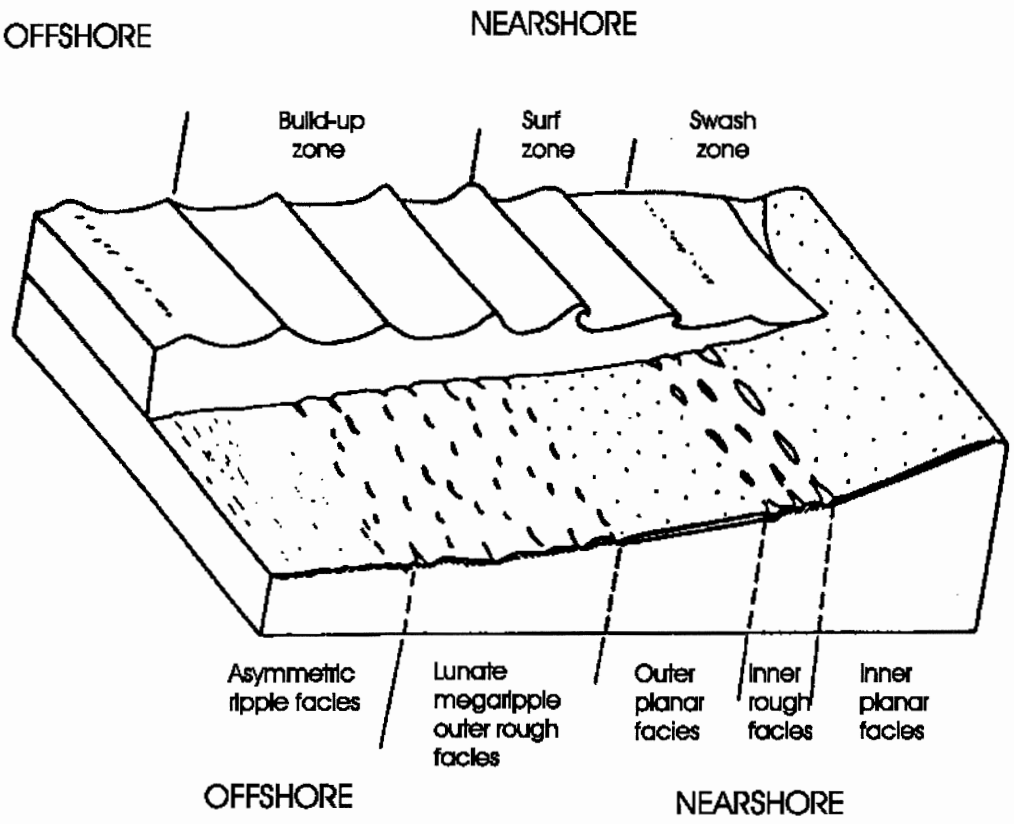

Figure 1.4 Five facies seen in the non-barred nearshore. Modified from Clifton et al., 1971.

Finally, the asymmetric ripple facies is profusely rippled with short-crested, wavy ripples whose crests are normal to the direction of the wave surge.

Clifton and Dingler (1984) looked at wave-formed structures and used these to reconstruct paleoenvironments. They determined flow parameters from the wave-formed features and then used these flow parameters to determine wave parameters and water depth. It was calculated that wave height and period can be determined from wave size and maximum wave period can be determined from orbital diameter and threshold velocity. Clifton and Dingler (1984) discussed four wave theories used to relate flow parameters to wave parameters: 1) The Airy theory used for small amplitude waves in all

water depths but not for asymmetric flows, 2) The Stokes theory which is inaccurate for large waves in shallow water but can be used for asymmetric flows, 3) The Cnoidal theory used for large waves in shallow water but very mathematically complex, and 4) Solitary waves used for progressive waves of a single crest.

Vincent and Osborne (1993) studied bedform dimensions and migration rates using high frequency acoustics. They concluded that two bedform types coexist under breaking waves; small ripples (0.5-2cm with wavelengths of 7-20cm) during low energy waves and high water, and large bedforms (3-8cm with wavelengths of 0.3-0.8cm) in more energetic waves in the surf zone. They also determined that small ripple migration rate depends on orbital excursion. By studying the effects of tides on oscillation ripples, Dingler and Clifton (1983) determined that ripple spacing and height respond to changes in orbital diameter only if the near bottom oscillatory flow is greater that the threshold velocity.

Hay and Bowen (1999) took measurements inside the breaker bar in the nearshore trough to study the migration rates of lunate megaripples. These bedforms were 1-5m long and 20-50cm wide. They migrated at speeds of 1-3m/hr in longshore currents of 20-80cm/sec and occurred as isolated units or with horns and crescents intersecting. Hay and Bowen (1999) found that migration rates and sediment transport depend on wave orbital velocity. Hay and Bowen (1993) used bedform migration rates to calculate bedload transport and discovered that ripple transport is not an important part of the local sediment budget and that bedform migration and suspended sediment can not be separated.

It is interesting to note the absence of any discussion on the presence of pock marks as a feature in the nearshore environment in any of the literature including such extensive compilations detailing bed features of all types as Allen's *Sedimentary Structures: Their Character and Physical Basis* (1982). There is mention in the literature of scour pits forming around small natural and man-made objects, which may bear some relation to pock marks (Allen, 1982b and Eadie and Herbich, 1986). Large pockmarks were also discovered on the Scotian Shelf by King and MacLean (1970) after the introduction of side-scan sonar and later found in the North Sea and Norwegian trench (Hovland, 1982). These large pockmarks are now known to occur on the continental shelf and slope and in the deep ocean (Hovland and Judd, 1988). King and MacLean (1970) described pockmarks on the Scotian Shelf as having a diameter of 14-45m and a depth of 5-10m. They hypothesized that these features were created by percolation of water or gas from underlying rock through the unconsolidated sediments above. They stated their age to be Holocene to Recent.

1.2 Thesis Objectives

This thesis has 5 specific objectives:

1) To determine the physical properties of pock marks such as size, shape, and their number density in $80m^2$.
2) To determine the time characteristics such as the lifetime, growth and decay rates, and migration rates.
3) To determine the hydrodynamic conditions for pock marks formation such as the flow energy and bottom shear stress.

4) To test the hypothesis that the presence of a nucleus is required for pock mark formation.
5) To document the genesis of lunate megaripples from pock marks.

1.3 Thesis Outline

In Chapter 2, the methodology of data collection is described. The SandyDuck97 experiment is explained indicating what the purpose of the experiment was, the location, and who were involved. The Canadian experiment is discussed describing what equipment was used and how and where it was set up, the hydrodynamic conditions over the course of the experiment, what data were collected, and the days and times that pock marks were observed. The data analysis methodology is described in a flow chart including projected dates of completion of each step.

Chapter 3 discusses the relationship of pock marks to hydrodynamics. This chapter will explain under what conditions pock marks form and how they affect sediment transport. Chapter 4 describes the pock marks themselves including physical and time characteristics, the presence or absence of an observable nucleus, and the instances of megaripple genesis from pock marks. The final chapter contains the summary and conclusions determined during the thesis as well as recommendations for future work.

Chapter 2: METHODOLOGY

Data used in this thesis were collected in August and November 1997 during the SandyDuck97 experiment. This chapter will describe the setting and aims of the SandyDuck97 experiment in general as well as explaining the specifics of the Canadian experiment including its goals, the equipment used, and the instrument setup. Information on the pock mark data collected from the fan beam images, such as appearance, time of occurrence, and hydrodynamic conditions, are introduced below and the methodology of the thesis is laid out in detail.

2.1 SandyDuck97

2.1.1 Overview

SandyDuck97 is the culmination of a series of experiments starting with DELILAH in 1990 whose purpose was to understand the sediment dynamics and hydrodynamics of the nearshore. DELILAH was followed in 1994 by Duck94 which tested new instruments and procedures in preparation for SandyDuck97. This final experiment involved 250 scientists from 26 international organizations (Table 2.1) conducting 30 different experiments related to the study of coastal sediment transport and the morphologic evolution in the nearshore (www.frf, 1997).

SandyDuck97 took place at the US Army Corps of Engineers Field Research Facility at Duck, North Carolina which lies on a barrier island running along North Carolina's Atlantic coast (Fig.2.1). The Field Research Facility is halfway between Cape Henry, 75km to the north, and Cape Hatteras, 75km to the south (Birkemeier et al., 1985).

Sponsors	US Army Engineer Waterways Experiment Station
	United States Geological Survey
	Office of Naval Research
Agencies	National Oceanic and Almospheric Administration
	Naval Research Laboratory
	Naval Postgraduate School
Universities	Dalhousie University (Canada)
	Duke University
	Memorial University of Newfoundland (Canada)
	North Carolina State University
	Oregon State University
	Scripps Institution of Oceanography
	State University of New York, Stony Brook
	University of California, Berkeley
	University of Deleware
	University of East-Anglia (United Kingdom)
	University of Florida
	University of Manitoba (Canada)
	University of South Florida
	University of Washington
	University of Wisconsin, Eau Claire
	Virginia Institute of Marine Science
	Washington State University
	Woods Hole Oceanographic Institution
Companies	Areté Associates
	Offshore & Coastal Technologies, Inc.

Table 2.1 SandyDuck97 Participants. Modified from www.frf, 1997).

The waves and currents at Duck vary by season. The average wave height is 0.9±0.6m with the lowest waves between April and September and the highest between October and December. Their approach is from the south in the spring and summer and there are extreme waves from the north between October and March (Birkemeier et al., 1985). The mid-surf zone currents vary in speed and direction with some periods of constant direction in the summer. Extreme surface currents up to 2m/sec occur during high waves and winds. There are also rip currents, low-salinity water masses, and Gulf Stream eddies present at Duck. The North Carolina coast is hit by extratropical and tropical storms but the Field Research Facility has the lowest hurricane occurrence on the east coast at 1 in every 42 years. The tides are semidiurnal and reach a height of 1m

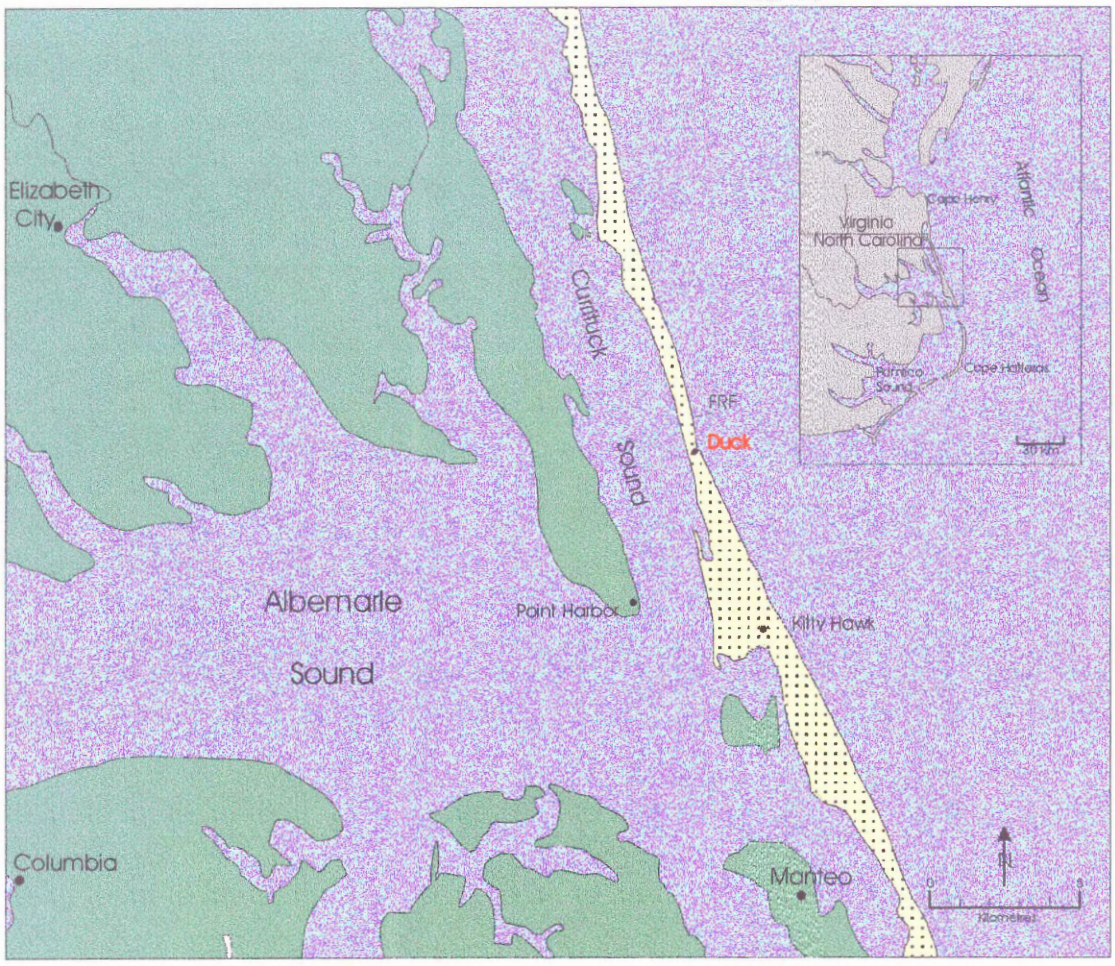

Figure 2.1 SandyDuck97 Location Map (based on www.frf, 1997).

(Birkemeier et al., 1985). During the 75 days of data collection, Duck experienced 12 small storms or forcing conditions and 1 major storm. The prevalent longshore current was to the north and the prevalent cross-shore current was to the west.

The barrier islands along North Carolina and Virginia's East Coast are comprised of Holocene sediments overlying Pleistocene deposits. Their origin is much debated. In the late 1800's, it was thought that these islands were from bar building or longshore drift and spit building (Birkemeier et al., 1985). Later, Hoyt (1967) suggested that transgression caused the flats behind the dunes to flood leaving behind an exposed ridge. Field and Duane (1976) thought the barrier islands formed during low sea level at which time barriers developed on the continental shelf. As sea level rose, the barriers were

pushed shoreward. There are still other views of submergence as their origin (Birkemeier et al., 1985). At the Field Research Facility location, the barrier island is 680m wide with a brackish water marsh on the landward side and dunes of up to 14m. Behind the beach are 7m high dunes and foreshore slopes up to 0.023-0.345°. The grain size of the sediments decreases landward from 0.52mm to 0.38mm. The foreshore sand becomes finer in the summer months while the dune sand remains the same all year at 0.3-0.4mm. The nearshore sediments are well-sorted, medium to fine-grained sand with an average grain size of 0.28-0.12mm. Finally, the sub-bottom sediments are interbedded coarse sands and gravels to well-sorted, fine sands. Below the sands are alternating silts, clays, and silty sands (Birkemeier et al., 1985).

2.1.2 The Canadian Experiment

The Canadian experiment had two main objectives: 1) To study the mechanisms involved in sediment suspension, and 2) To determine bedform sizes, genesis rates, and migration rates. The instruments used in this experiment were a rotary fan beam sonar with a 5m range and a rotary pencil beam sonar with a 5m range and oriented to image a vertical slice in the on-offshore plane, and operated in fixed up and down looking and sector modes as well as the full 360° rotation. An acoustic coherent Doppler profiler, pressure and temperature sensors, and dual axis tilt sensors were also deployed along with Marsh-McBirney electromagnetic and Sontek single-part acoustic Doppler flowmeters to take horizontal

Figure 2.2 CRAB used to deploy instruments (based on www.frf, 1997).

velocity measurements. Video cameras were mounted on high towers in order to obtain images of breaking waves and surface foam (www.frf, 1997).

The Coastal Research Amphibious Buggy (CRAB), developed by the US Army Corps of Engineers, was used to deploy the equipment (Fig.2.2). CRAB is an aluminum tripod with an operation platform 10.7m off the ground. It uses a Volkswagen diesel engine for power and can move at 3.2km/hr. The vehicle weighs 8,200kg and its water filled tires make it very stable. It can not be used in soft, silty, or loose bottoms (www.frf, 1997).

2.2 Instrument Locations

The instruments for the Canadian experiment were mounted on metal frames and set up in an L-shaped array (Fig. 2.3 and 2.4). The cross-shore consisted of 4 frames and the longshore of 3 frames, all of which had spacings of 20-60m and were at a depth of approximately 3m with a 1 m tidal range. All frames were equipped with pressure and flowmeter sensors, rotary side scan sonar used to measure bedform pattern and relief within a 10m diameter, and two-axis tilt sensors used to correct frame attitudes of bottom images. Hydrophones and upward looking sonar were mounted on Frames B, C, and D, and Frame A contained the coherent Doppler profiler. The data studied in this thesis is mainly fan beam and pencil beam sonar images from Frame C. The characteristics of the rotating sonar are seen in Table 2.2.

	Fan Beam	Pencil Beam
Frequency	2.25 MHz	2.25MHz
Vertical beamwidth	30degrees	10degrees
Horizontal beamwidth	0.8 degrees	1 degrees
Pulse duration	10 microseconds	10 microseconds
Range resolution	0.9cm	0.9cm

Table 2.2 Rotating Sonar Characteristics (Modified from Hay and Bowen, 1999).

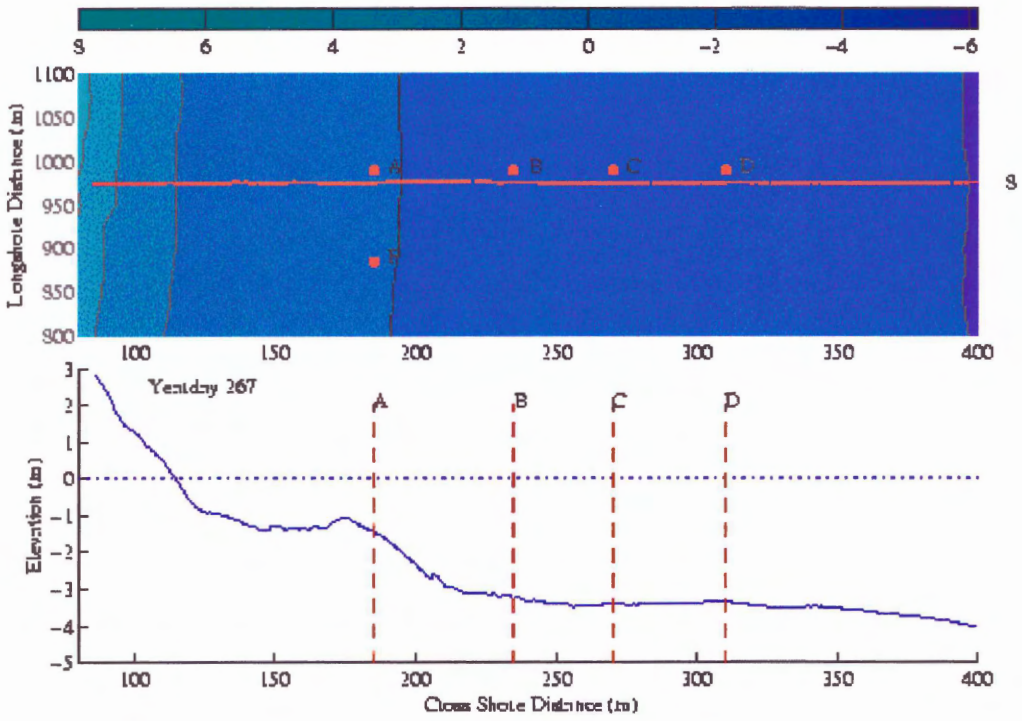

Figure 2.3 Top image shows a plane view of the instrument array. Bottom image shows a bed profile for yearday 267. Note that frame C is at a depth of approximately 3m.

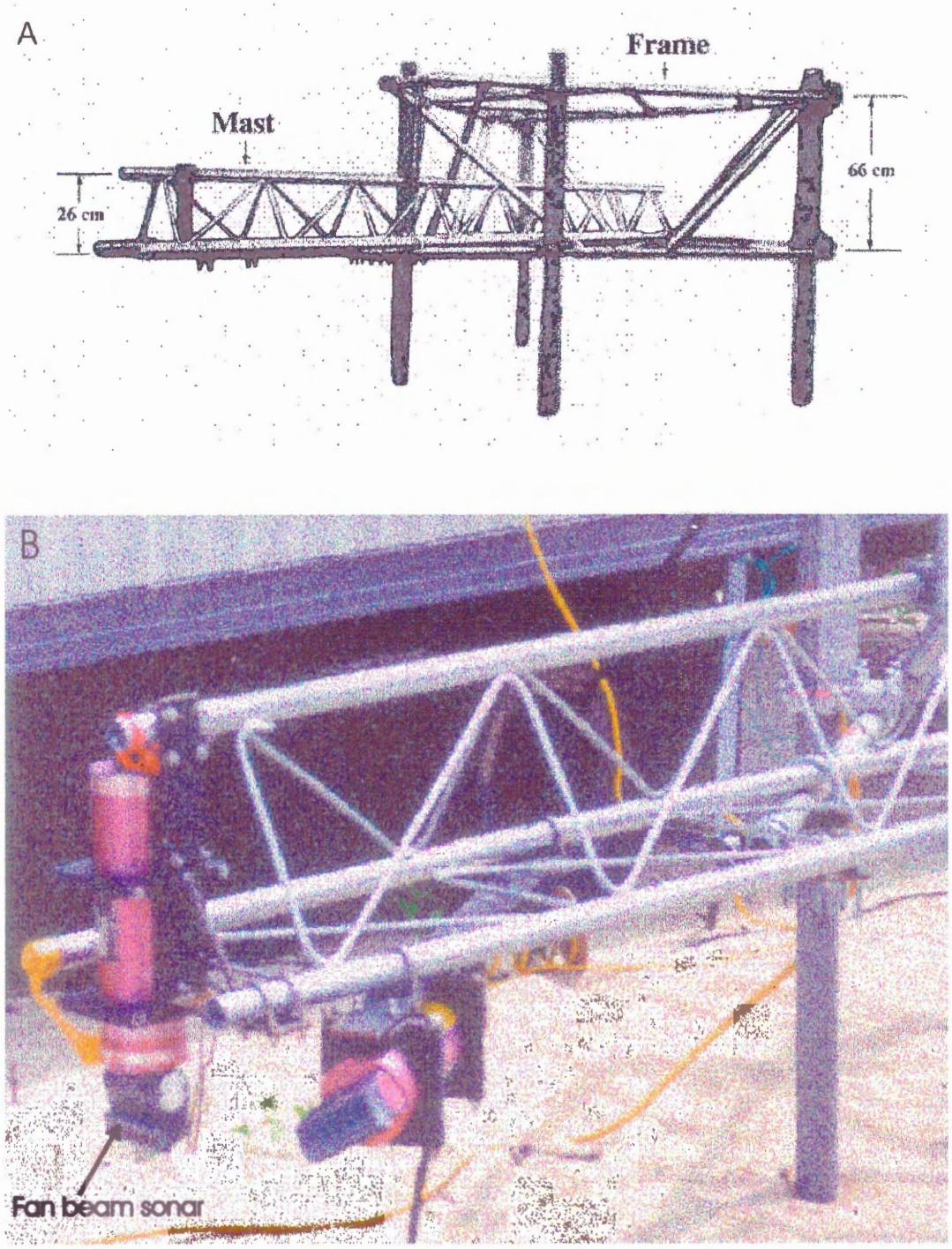

Figure 2.4 A) Schematic of a metal instrument frame. B) One of the actual frames deployed during SandyDuck97 with a fan beam sonar attached.

2.3 Methodology

Using the fan beam sonar images, the Dalhousie Ocean Acoustic Lab created movies tracking the movement of bedforms across the seafloor in time intervals of 10 minutes or 0.008 yeardays. These movies were viewed using the computer program XAnim with pock marks appearing as circular depressions of a darker colour than the surrounding area (Fig.2.5). The pock mark occurrences were documented in a database showing their start and stop times in both yeardays (the number of the day out of 365 and the time, i.e. January 15, 7:00pm appears as "015 15:00") and file numbers (isums), how many were present over a period of time, their general size, if they were migrating or forming and disappearing quickly (giving them a twinkling appearance), and if they formed megaripples (Appendix B).

Times were selected from the movies that contained an abundance of distinct pock marks which could be used as a basis for extracting quantitative information such as size and shape. Individual pock marks from these times were captured as subimages and imported into Matlab which was then used to make quantitative measurements of the subimages (perimeter, area, etc) using an edge detection algorithm. This information was put into a database of pock mark characteristics and combined with the hydrodynamic database already created to determine the quantitative relationships between the forcing conditions and the pock marks. A flow chart of the methodology can be seen in Figure 2.6.

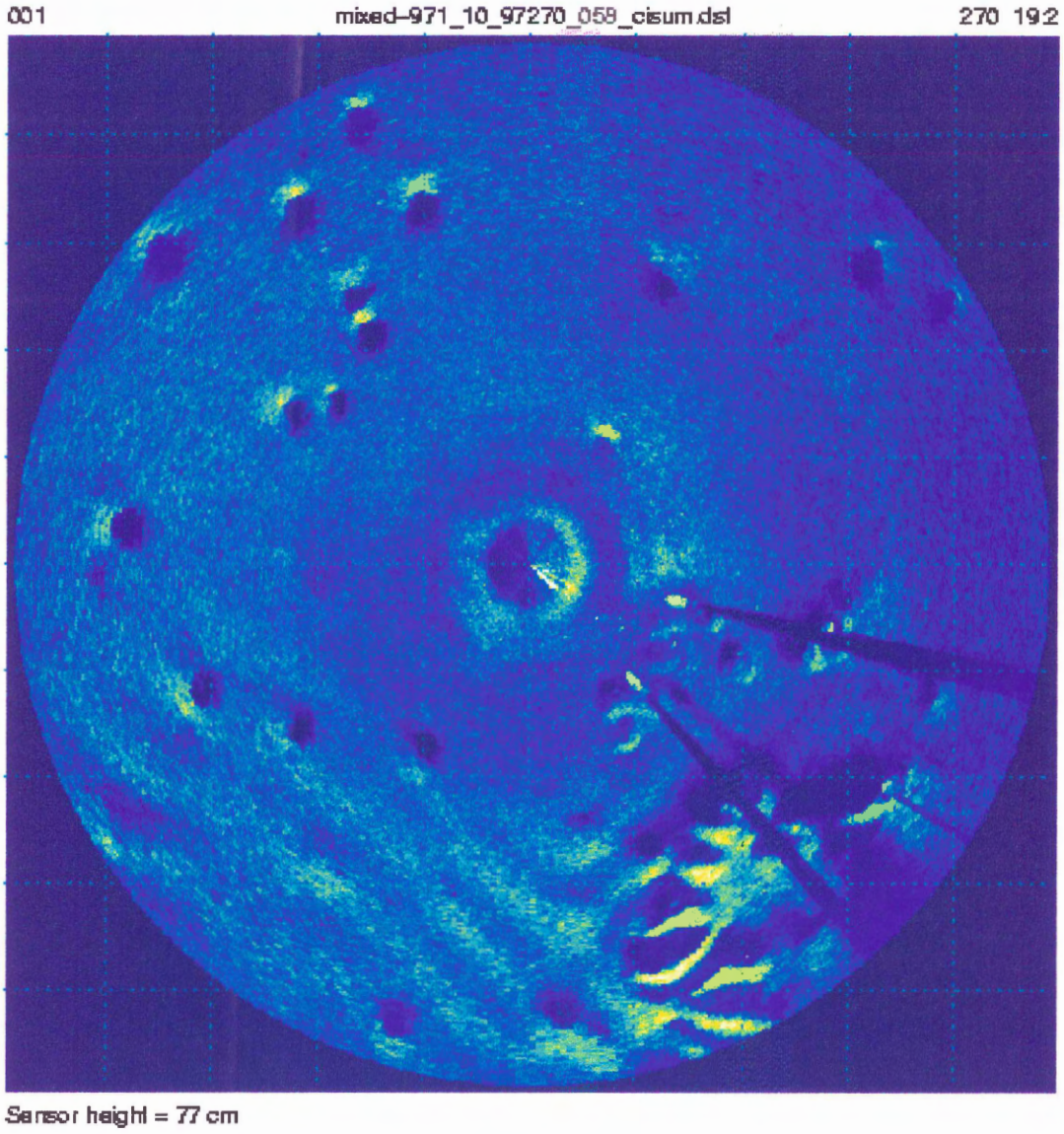

Figure 2.5 Fan beam image with pock marks appearing as dark blue circles. In this image, the pock marks appear simultaneously with linear ripples. Also seen are the shadows from the legs of the instrument frame and the sandy patch surrounding the legs containing a high density of large bedforms. Note that one box is $1m^2$.

2.4 Data Set

During the 3-month experiment, fan beam images were taken every 10 minutes. Of these, 189 fan beam images have been analyzed from 8 pock mark episodes between yeardays 264 and 275. In the 8 days, 1000 subimages of pock marks were captured representing 138 different pock marks. Appendix A shows which pock marks occurred at each time within the 8 episodes and their locations on the fan beam image. In this thesis, all pock marks are included in the statistics. It is possible, however, that the regions around the legs of the instrument frame have an effect on the formation of pock marks and should be excluded. This is under investigation. Table I-9, in Appendix A, shows the pock marks that may be affected by the frame.

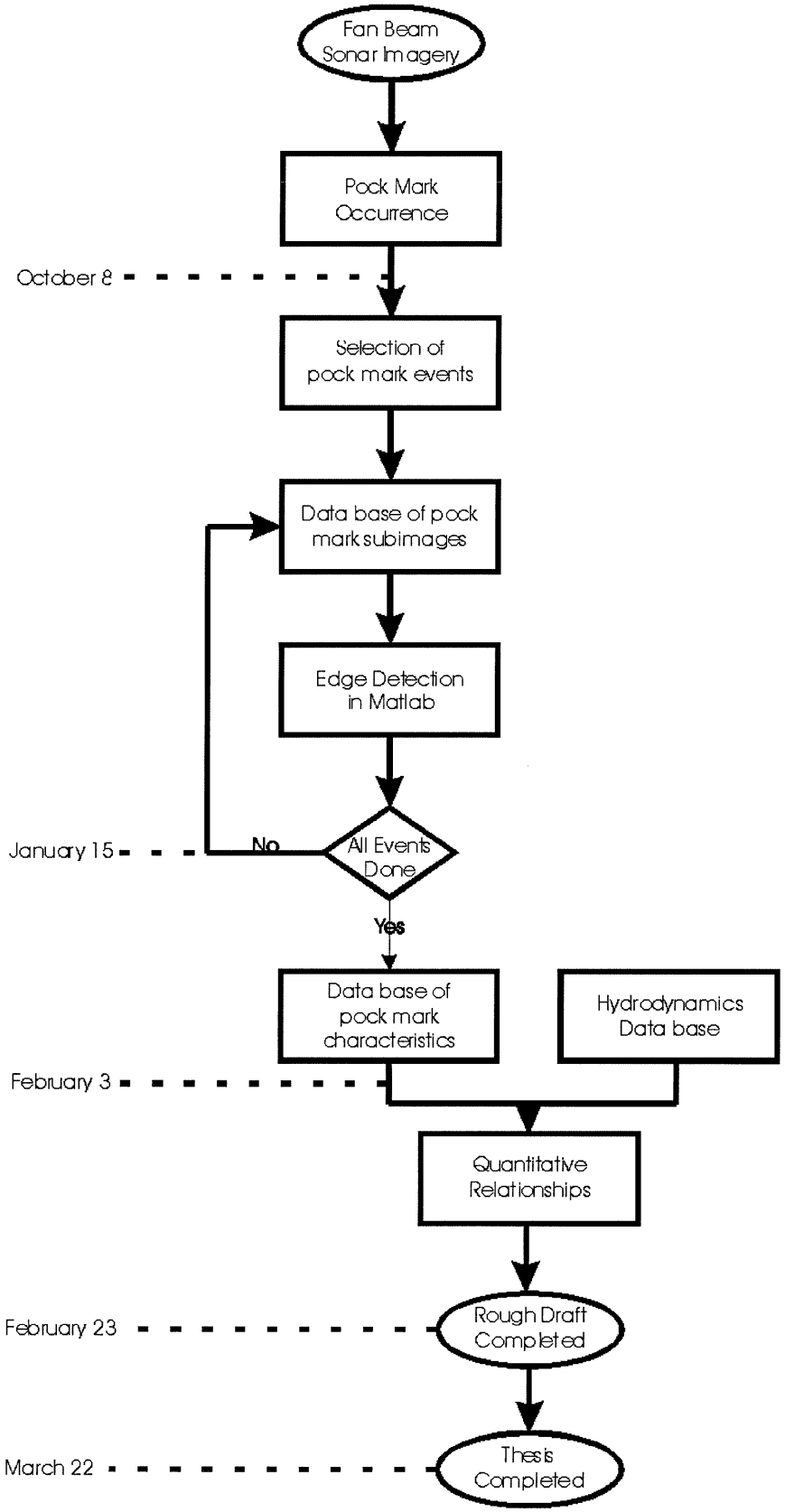

Figure 2.6 Flow chart showing methodology of the thesis.

Chapter 3-RELATIONSHIP TO HYDRODYNAMICS

True to Hay and Wilson's (1994) experiment, at SandyDuck97 the seafloor under the instruments showed a wide range of bedform types throughout the progression of a storm event from cross-ripples to flatbed. Of the pock marks studied between yeardays 264 and 275, those in the growth phase of a storm occurred just after irregular or linear ripples with some pock marks forming on the slope of the ripples near the crest. In some of these cases pock marks occurred simultaneously with linear ripples and lunate megaripples but most occurred on a flat bed. Those pock marks which formed during storm decay all formed directly after flat bed conditions and were followed by irregular beds.

3.1 Existence Conditions for Pock Marks

When looking at the individual forcing conditions that could affect the formation of pock marks, cross-shore mean current, longshore mean current, and wave orbital velocity were all studied (Fig.3.1). Figure 3.1 indicates that pock marks occurred in a wide range of cross-shore mean currents from +2cm/s to15cm/s and in both positive and negative longshore mean currents. Pock marks did not occur, however, when the mean longshore currents were strong (>50cm/s). Longshore mean current did have an influence on the direction of pock mark migration as seen in section 4.2.2. From Figure 3.1 it is apparent that pock marks occur in a distinct range of wave orbital velocities from 50 to 115cm/s but occur during positive, negative, and zero values of cross-shore mean and longshore mean currents. This indicates that wave orbital velocity had the greatest effect on the formation of pock marks.

Over the full data set, pock marks formed during all of the 13 storm events and in all but one event, for which a pock mark occurred at its peak, pock marks appeared during both storm growth and decay. During storm growth, pock marks tended to occur just before flat bed, and during storm decay, just after flat bed. This indicates that pock

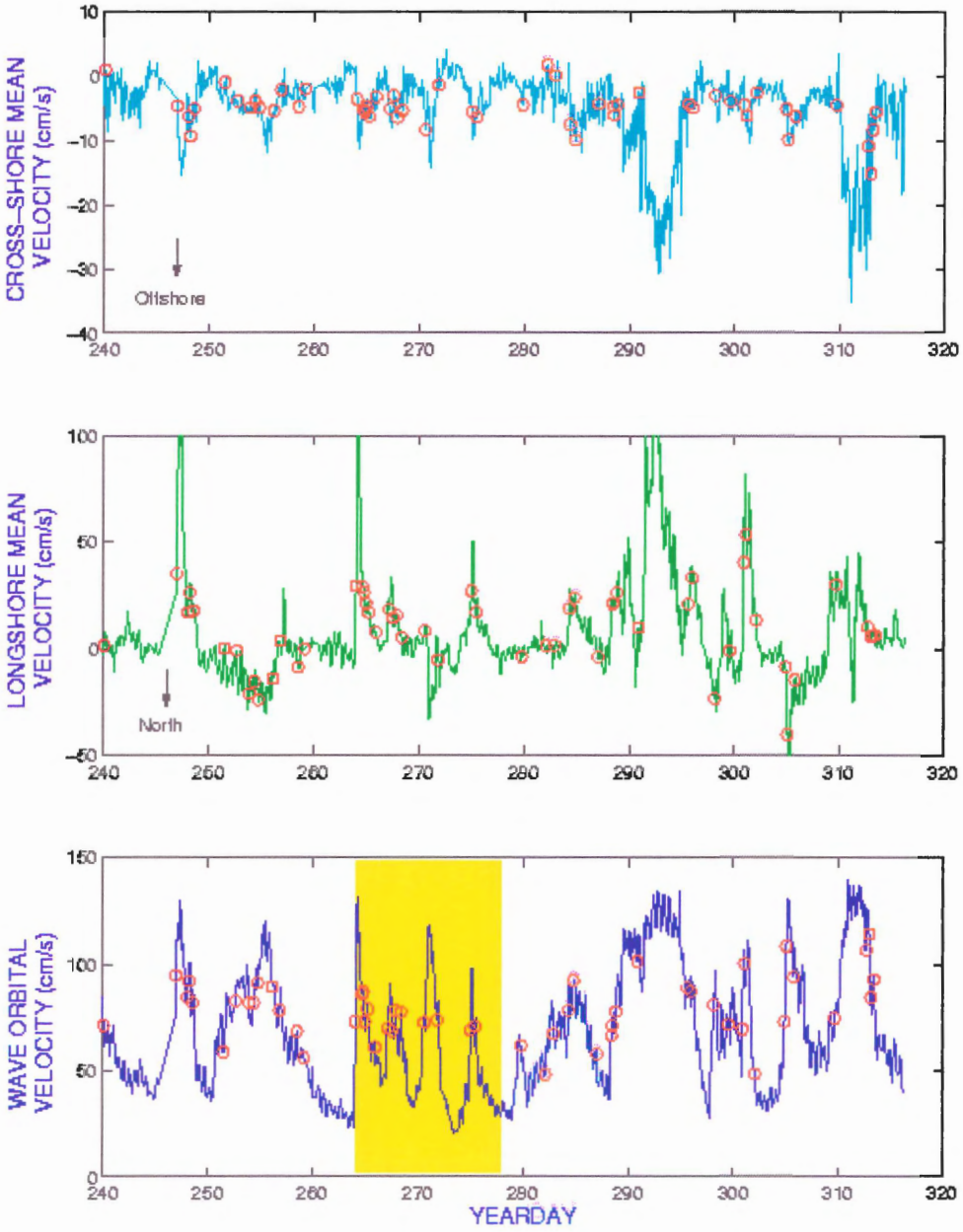

Figure 3.1 Graph of the hydrodynamic conditions during SandyDuck97 and their relationship to pock mark occurrence. Yellow shaded area represents the yeardays pock marks have been analyzed. Red circles = pock mark occurrences.

marks do not necessarily form as a result of bed roughness associated with previous bedforms (i.e. linear or cross ripples as they also form after a flat bed.

Over the 75 days, pock marks occurred between a range of wave orbital velocities of 50-115m/s (Fig.3.1). The data analyzed during yeardays 264-278 illustrate the same pattern of pock mark occurrence and a range of wave orbital velocities between 60 and 80cm/s (Fig.3.2). When the number of pock marks is added to the plot, it appears that slightly more pock marks occur as the storm is ramping up than as the storm is ramping down. A graph of the frequency distribution of the pock marks at specific wave orbital velocities again clearly displays the range of velocities in which pock marks formed at Frame C, between 60 and 100m/s with a mean of 75cm/s (Fig.3.3).

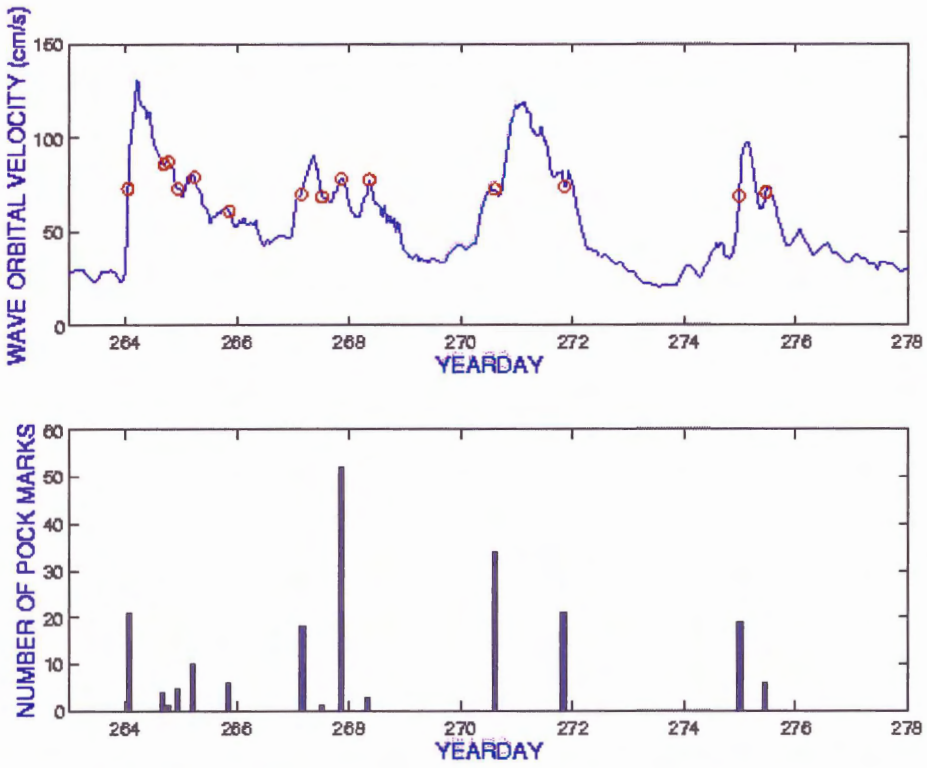

Figure 3.2 Graph showing the hydrodynamic conditions and number of pock marks during SandyDuck97. Red circles = pock mark occurrences.

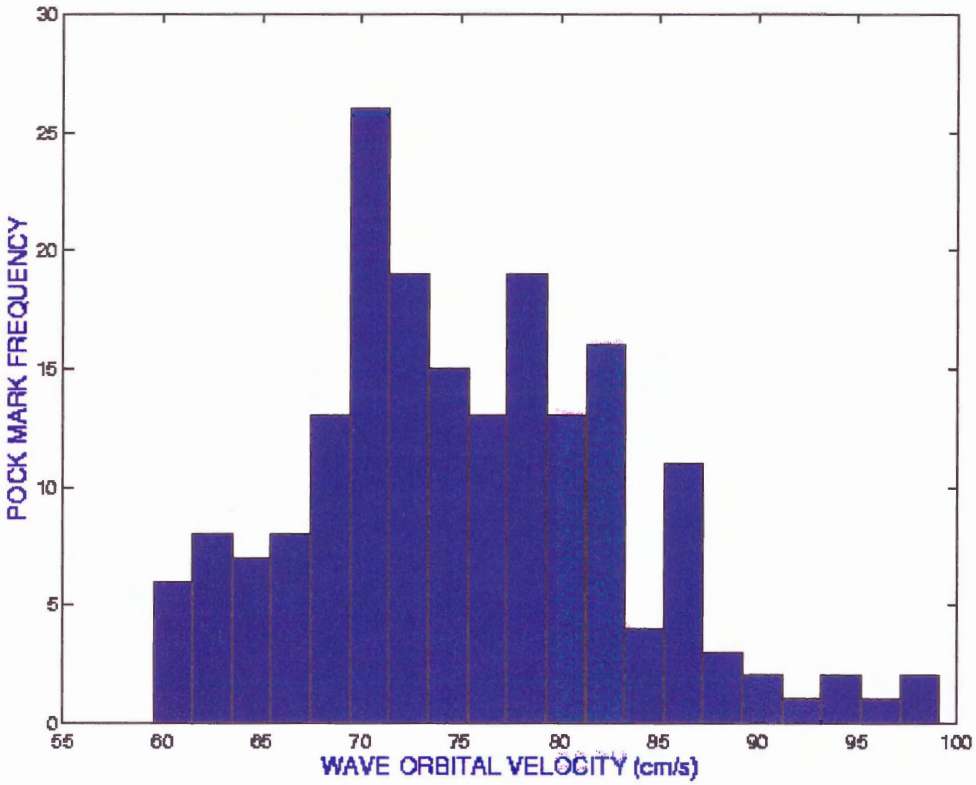

Figure 3.3 Graph of the frequency distribution of pock marks at specific wave orbital velocities.

Combining cross-shore mean, longshore mean, and wave orbital velocities into total kinetic energy shows that pock marks occur in a wide range of energies between 2500cm^2/s^2 and 15000 cm^2/s^2 (Fig.3.4). Again, there is a distinct threshold energy, above which pock marks do not occur. Taking the square root of the total kinetic energy gives a range of 50cm/s to122cm/s which corresponds well with the wave orbital velocity range and thus supporting the inference that wave orbital velocity is a primary forcing parameter affecting pock mark formation.

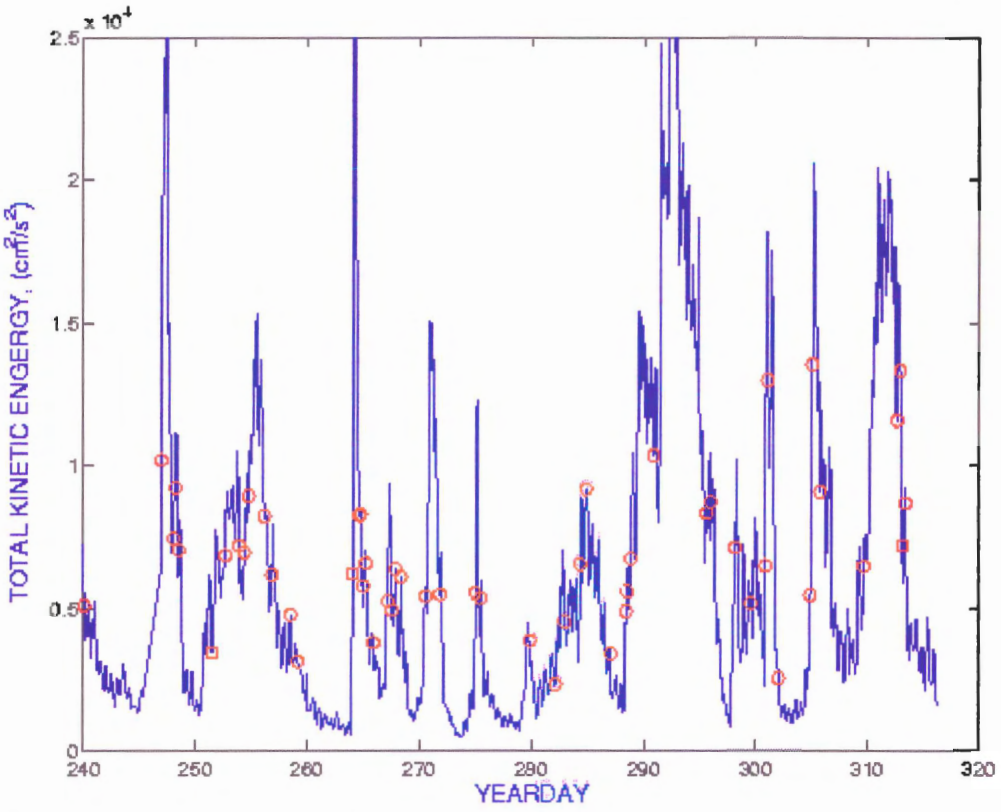

Figure 3.4 Graph of the total kinetic energy during SandyDuck97 and its relationship to pock mark occurrence. Red circles = pock mark occurrences.

Chapter 4: POCK MARK CHARACTERISTICS

Data collected from the fan beam sonar were processed in three Matlab programs. The first was used to extract subimages of individual pock marks from the whole fan beam sonar image. This was done for a number of different time series throughout the 75-day period. In a fan beam sonar image, a pock mark is indicated by an approximately circular region of low acoustic backscatter, corresponding to a local depression in the seabed. The second Matlab program identified the outline of the pock mark's shadow using an edge detection algorithm. The third program was then written to convert these shadow outlines to quantitative pock mark properties: area, diameter, and centroid position. These properties were used to determine the migration patterns and rates.

4.1 Physical Characteristics

4.1.1 Pock Mark Shape and Size

The shape of the pock marks was obtained visually by studying the fan beam sonar images. Most were determined to be approximately circular while some appeared to be slightly elongated and more elliptical.

The diameter of those pock marks formed during storm growth had a mean and estimated mode of 19cm and a median of 18cm (Fig.4.1) while the diameter of those formed during storm decay had a mean and estimated mode of 14cm and a median of 13cm (Fig.4.2). This indicates a tendency for pock marks to be larger during storm growth than storm decay. This conclusion may be slightly biased, however, as the diameters during storm growth include pock marks in the lunate megaripples stage.

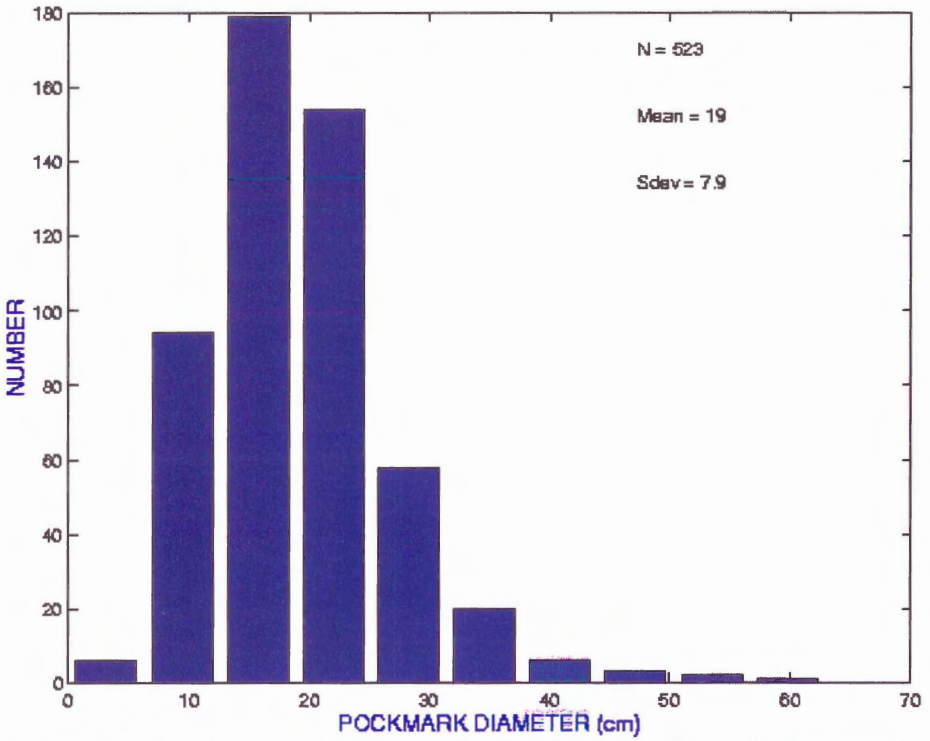

Figure 4.1 Graph of the frequency distribution of pock mark diameter during storm growth.

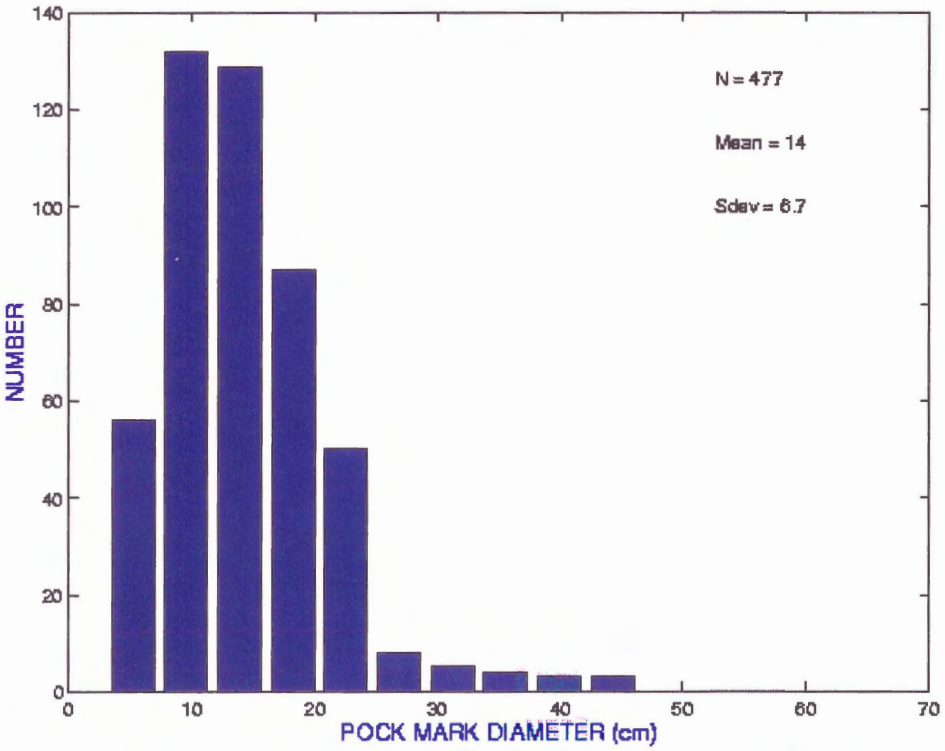

Figure 4.2 Graph of the frequency distribution of pock mark diameter during storm decay.

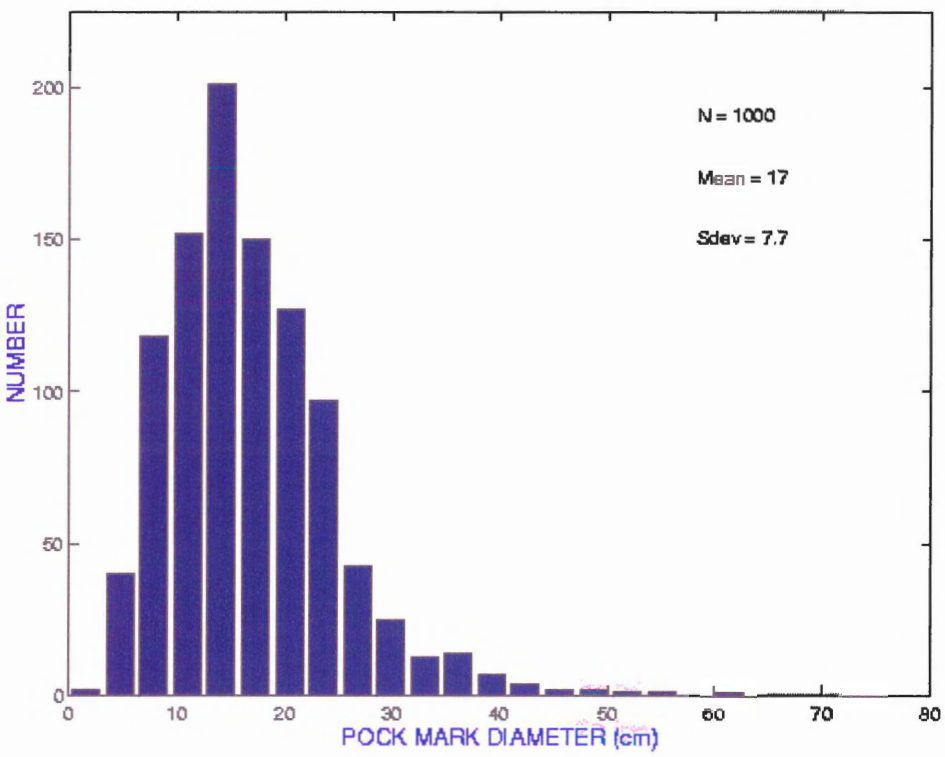

Figure 4.3 Graph of the frequency distribution of pock mark diameter during both storm growth and decay.

The total diameter of all the pock marks seen on the analyzed yeardays varied from 4cm to 65cm and had an average diameter of 17cm (Fig.4.3). (It should be noted that the largest diameters here include those features which developed into lunate megaripples and may not represent individual pock marks). Pock mark area varied from 7cm^2 to 3100cm^2 and had a mean of 270cm^2. Individual pock marks were observed to go through varying growth and decay patterns during this time.

4.1.2 Pock Mark Depth

The depth of the pock marks was determined in two ways: From the angle of repose, and from the pencil beam bed elevation profiles.

Eadie and Herbich (1986) performed a laboratory experiment on scouring at the base of a cylindrical pile 1.5 inches in diameter under combined waves and currents.

Once the final scour depth was reached, the slopes were at the angle of repose. For this study a simple calculation was made using 17cm as the average pock mark diameter and 23° as the "residual angle of shearing (Φ_r)", which gives the angle of the slope after avalanching has stopped, and 33° as the "angle of initial yield (Φ)" (Sleath, 1984). The calculation using Φ_r indicated that the depth of the pock marks 17cm in diameter should be no more than 7.2cm while using Φ gave a depth of 11cm.

Next, the pock mark movies were viewed in order to identify pock marks that occurred on the line of the pencil beam sonar. Only five such pock marks were formed, with approximate diameters (from the fan beam images) of 10-15cm. The pencil beam profiles for these pock marks gave an approximate average depth of 3cm (Fig.4.4). It is important to note that the diameter determined using the edge detection algorithm on the fan beam data was 15-20cm but Figure 4.4 shows the same pock marks as having diameters of approximately 45cm. This indicates that the edge detection algorithm actually gives diameters which are biased toward of the deepest part of the depression, and that the actual diameters of the negative relief depressions may be approximately 2 times larger than in Figures 4.1-4.3.

The depths determined using the pencil beam data might be affected by acoustic shadowing of the bottom of the depression by the edge (Fig.4.5). This depends on the geometry and the exact angle of repose of the features. The equation

$\mathbf{(Z'/ Z_P) = 2/[1+(\tan\beta/\tan\theta)]}$ illustrates this relationship.

From this equation it is determined that an angle of repose of 23° gives a depth 20% smaller than the actual depth and an angle of repose of 33° gives a depth 30% smaller.

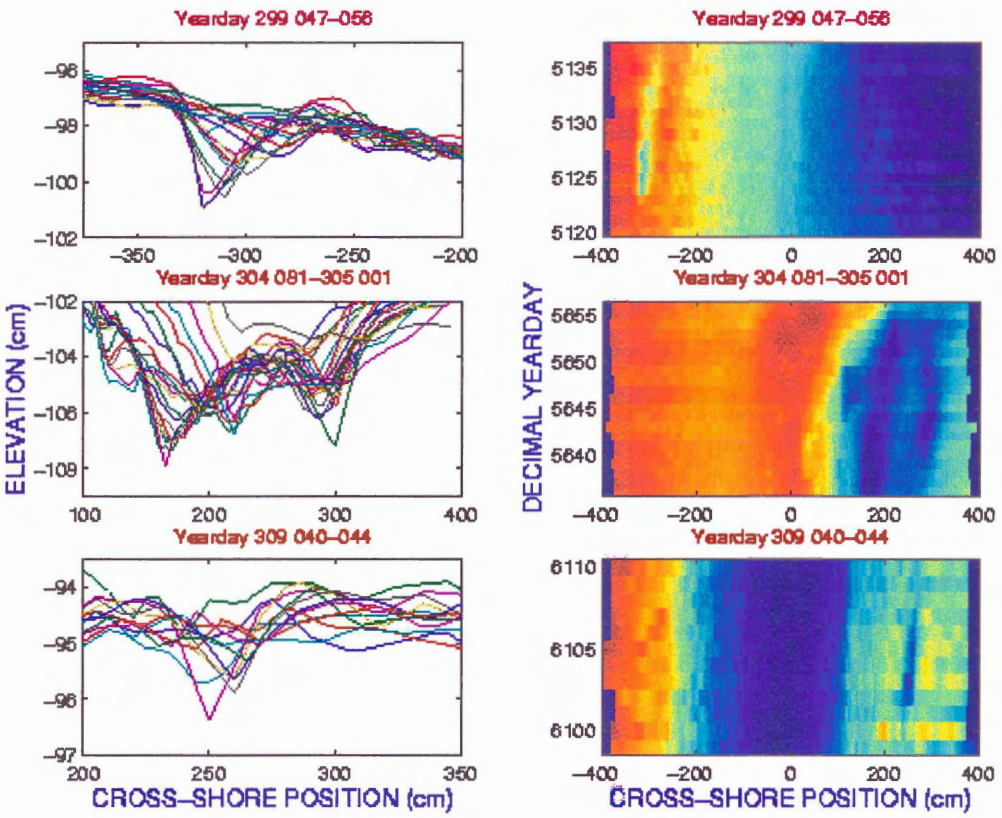

Figure 4.4 Depths of the pock marks determined by pencil beam images. Linear images show the elevation of pock marks (approximately 10-15cm in diameter) through time. False colour images show pock marks as dark blue (negative relief) colours migrating through time. The top images have a pock mark at –300cm, the middle images at 175cm, and the bottom images at 250cm.

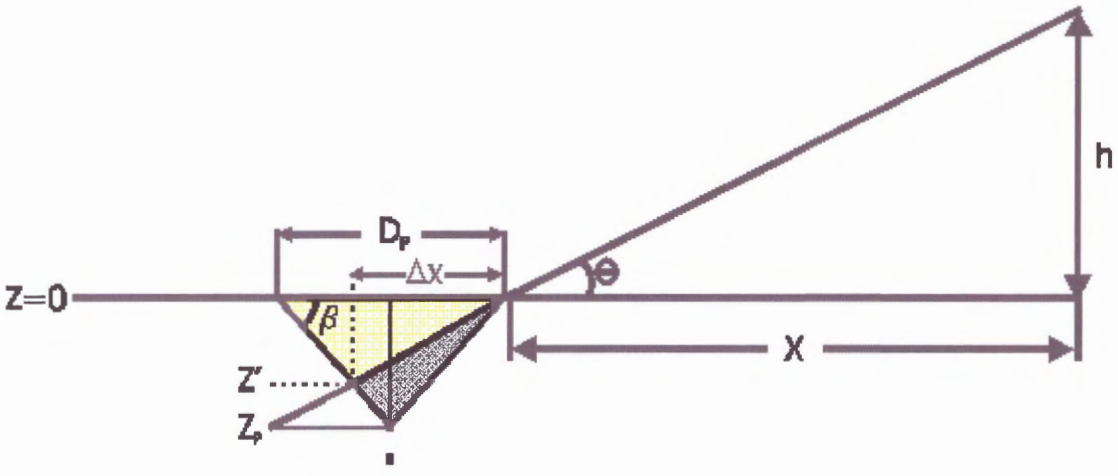

Figure 4.5 Schematic diagram of acoustic shadowing where yellow shading indicates the actual pock mark size and grey shading indicates the part of the pock mark not seen by the fan beam sonar. D_P = Pock mark diameter, Z_P = Pock mark depth, x = distance from the instrument to the pock mark, and h = instrument height.

4.1.3 Number Density of Pock Marks

For the analyzed yeardays 264-278 there was a range of 1 to 22 pock marks appearing at the same time in the fan beam image of $80m^2$. The mean number density of pock marks throughout this time was $5/80m^2$. For the 75-day period of data collection, when pock marks were present there were as few as 1 and as many as 30 individual pock marks within this area at any one time (Appendix B). The mean number density during the 75 days was $4.5/80m^2$.

4.2 Time Characteristics

4.2.1 Group Lifetime, Growth and Decay

Although the appearance of individual pock marks in the fan beam images is random, their lifetime was measured in groups from the time the first pock mark appeared until the last disappeared. This group lifetime of pock marks for the entire data set varied from 0.3h to 30.2h and had a mean of 4 hours (Appendix B). Within the analyzed data, the group lifetime ranged from 0.2h to 9h and there was a mean of 4.5h. Since pock marks were only included in the statistics if they remained in the fan beam image for more than one frame (or 10 minutes), it is possible that the group lifetime could be shorter. Also, lunate megaripples that formed from pock marks were included in the statistics which may give a longer group lifetime than is actually present. The scours formed in Eadie and Herbich's (1986) experiment were quick to develop with the scour pattern beginning to form almost immediately at 2-5 minutes and being well developed by 30 minutes after the start of a run. The scour reached its maximum depth by 2-3h. These time scales are similar to the ones seen in the SandyDuck97 pock mark formation.

Between the yeardays 264 and 275, pock marks changed in size in a number of ways. Some decayed in diameter, some went through a growth and decay cycle, others decayed and then grew, and finally some appeared to go through a growth-decay-regrowth cycle.

4.2.2 Pock Mark Migration

The migration of pock marks appeared to be in the onshore direction, moving with the wave direction, and was affected by the longshore mean current (Fig.4.6). Of the eight episodes analyzed, four (264.05-264.07, 264.64-264.73, 267.08-267.27, and 274.96 –275.02) migrated with the longshore current to the south, three (267.69-268.06, 270.39-270.86, and 271.67-271.99) remained stationary due to the longshore current being very weak, and one (275.34-275.47) appeared to migrate against the longshore current to the north. The rate of migration has yet to be determined.

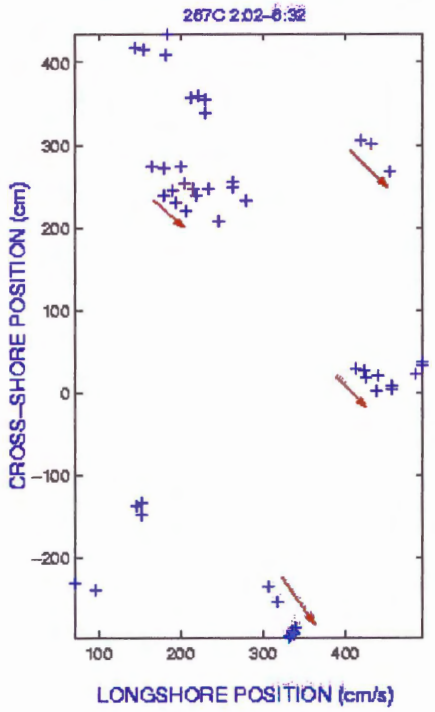

Figure 4.6 Graph showing the migration pattern of yearday 267.08-267.27. Note the pock marks are clearly migrating onshore and to the south (right) as influenced the longshore current. The y-axis reflects the pock mark location with respect to their position in the fan beam image where 0 = the center of the image.

4.3 Presence of a Nucleus

Whether or not pock marks contain a nucleus is important in relation to possible modes of formation. The presence of a nucleus could indicate a scouring action around a shell or pebble. After the storm events at SandyDuck97, pebbles and shells of 5-10cm were washed up on the beaches, as well as large conch shells of >20cm, indicating the presence of such potential nuclei. Also, Schwartz et al. (1997) studied vibracores from the area north of the pier at Duck, N.C. that contained gravel zones with scattered pebbles, another possible nuclei source. Allen (1982b) states that the diameter of a scour around cylindrical pilings is 3-5 times the diameter of those pilings. By analogy then, the diameter of the nucleus within a 17cm pock mark should be 3-5 times smaller than the pock mark diameter or 3-5cm (Fig.4.7). Figure 4.8 follows the movement of Pock Mark A on yearday 264c. Within the core of the pock mark a nucleus with an approximate diameter of 5cm can clearly be seen. According to Eadie and Herbich (1986), the diameter of the scour around a cylindrical piling depends on wave orbital velocity and time, and therefore not on piling diameter alone. They found that the scour reaches its maximum size 2-3 hours after its initiation, and scour diameter increases with increasing wave orbital velocity. This indicates that the size of the nucleus in a pock mark is not uniquely related to pock mark diameter, and that the 3-5cm range obtained above based on average pock mark size should be regarded as a rough estimate.

Of the 1000 fan beam subimages analyzed, 112 contained a nucleus. This represents 12 of the 138 total pock marks. Although this appears to be only a small percentage, it is possible that the nuclei are either too small, too flat, or too deep in the depression for the sonar to detect (9 of those 12 pock marks occurred 4+ meters away

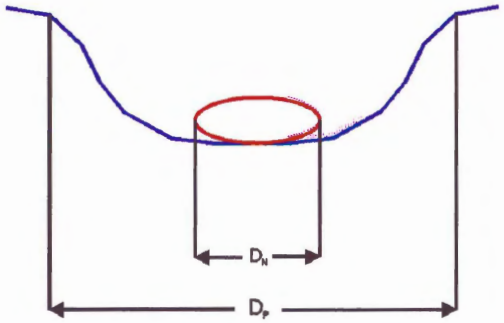

Figure 4.7 Diagram showing the relationship of pock mark diameter to nucleus diameter where D_N = Nucleus Diameter and D_P = Pock Mark Diameter.

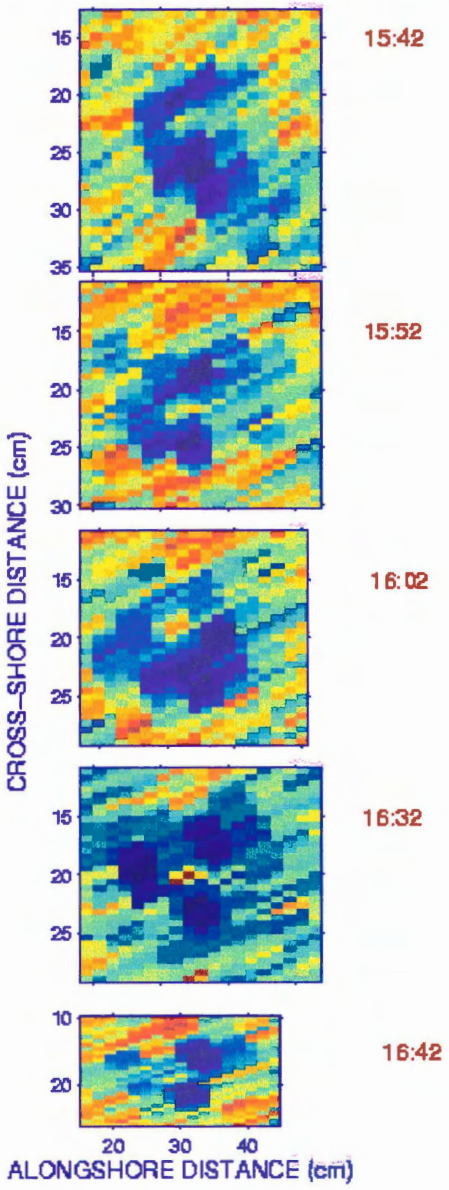

Figure 4.8 Image showing pock mark 264c-I with a nucleus migrating through time.

from the sonar where more of the pock mark is affected by acoustic shadowing) (Fig.4.5). Further study of detecting nuclei within pock marks will be conducted under controlled conditions.

Table 4.1 gives a summary of all the physical characteristics of the pock marks for each of the eight time series analyzed.

						# of Nuclei in		Formation
Yearday	Mean Diameter	Sdev	Mean Area	# of PM	# Distinct PM	Subimages	Distinct PM	into LM
264.05-264.07	17	5.6	246	43	21	N/A	N/A	YES
264.69-264.73	17	6.7	251	16	4	8	2	NO
267.08-267.27	22	15	543	53	18	2	1	YES
267.69-268.06	16	7.4	240	270	52	52	3	NO
270.39-270.86	19	7.3	336	379	34	21	3	NO
271.67-271.99	11	3.9	110	153	21	28	2	NO
274.96-275.02	16	5.5	234	48	19	N/A	N/A	NO
275.34-275.47	14	5.9	188	38	6	N/A	N/A	NO

Table 4.1 Physical characteristics, by time series, of all pock marks analyzed.
PM = Pock Mark LM = Lunate Megaripple.

4.4 Megaripple Formation

There are 6 instances in the 75-day pock mark data set in which lunate megaripples developed from pock marks within the range of the sonar. In some of these instances, more than one pock mark developed into a lunate megaripple. There were also four cases in which lunate megaripples occurred simultaneously with pock marks but entered the sonar field already fully developed (2 cases existed when lunate megaripples migrated into the sonar field fully developed with no pock marks present). In these last instances, the lunate megaripples may have developed from pock marks before entering the sonar's range.

Of the six instances where pock marks developed into lunate megaripples, five occurred at Frame C on yeardays 237.82-238.31, 246.83-246.88, 251.40-251.46, 264.05-264.07, and 267.08-267.27, and one occurred at Frame D on yearday 300.90-300.98.

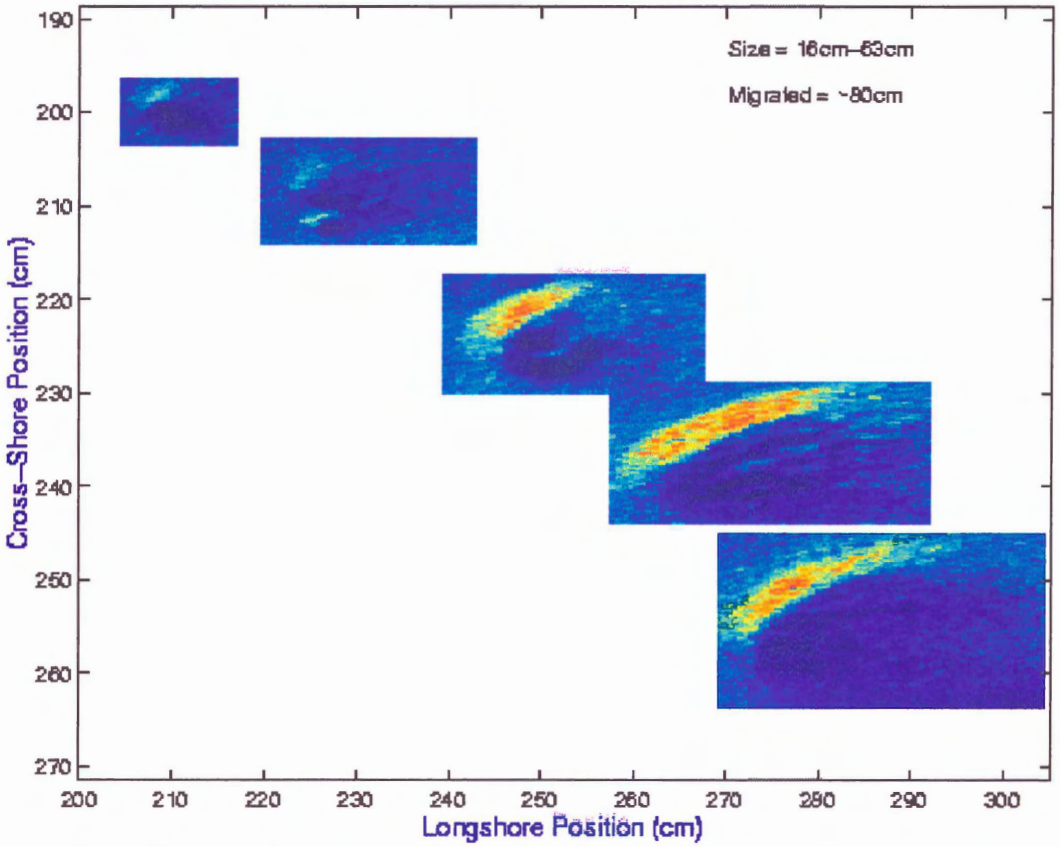

Figure 4.9 Formation of lunate megaripple from pock mark 267C-I where the upper left image is the earliest in the sequence and the lower right image is the latest. This feature is migrating onshore (down) and to the South (right).

Figure 4.9 shows a time sequence of subimages for Pock Mark I on yearday 267.08-267.27 as this pock mark migrates onshore and becomes a lunate megaripple. The pock mark increased in diameter from 16cm to 63cm. As it grew, it migrated onshore and to the south approximately 80cm. Also seen in Figure 4.9 is the clear development of a high backscatter feature (in yellow) which lengthens over time and becomes slightly curved. In all cases, the lunate megaripples migrated onshore as they developed with the high backscatter feature forming on the offshore margin of the megaripple pit in all but two cases.

Wave-formed lunate megaripples, like pock marks, are primarily negative relief

features on the seafloor (Hay, 2000). It is thought that one mechanism by which pock marks form is due to water impinging on the wall of a slight irregularity or nucleus in the seafloor creating enough torque to form a vertical vortex. This vortex reverses direction with the wave and scours out a pit in the seabed (Fig.4.10). If the depression becomes large enough, a horizontal vortex can form at the edge of the pit. This horizontal vortex begins to erode the sides of the pock mark creating a more elongated and curved feature. Eventually the horns of a lunate megaripple appear and sediment thrown up by the horizontal vortex forms the ripple ridge that is now apparent (Hay, 2000) (Fig.4.11). The exact hydrodynamic conditions under which this occurs has yet to be determined but it is known that all the instances of pock marks developing into lunate megaripples occurred during the growth phase of a storm.

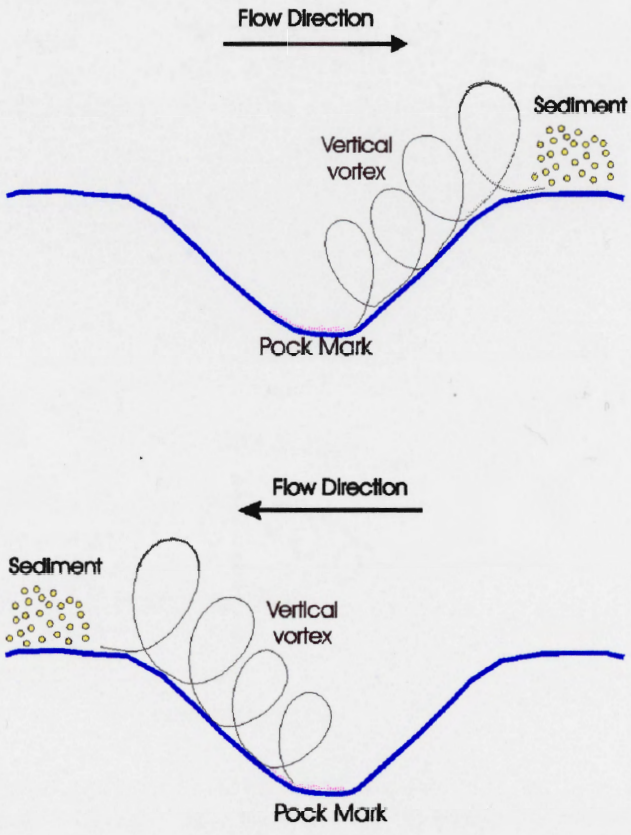

Figure 4.10 Schematic diagram showing the formation of a pock mark by a vertical vortex.

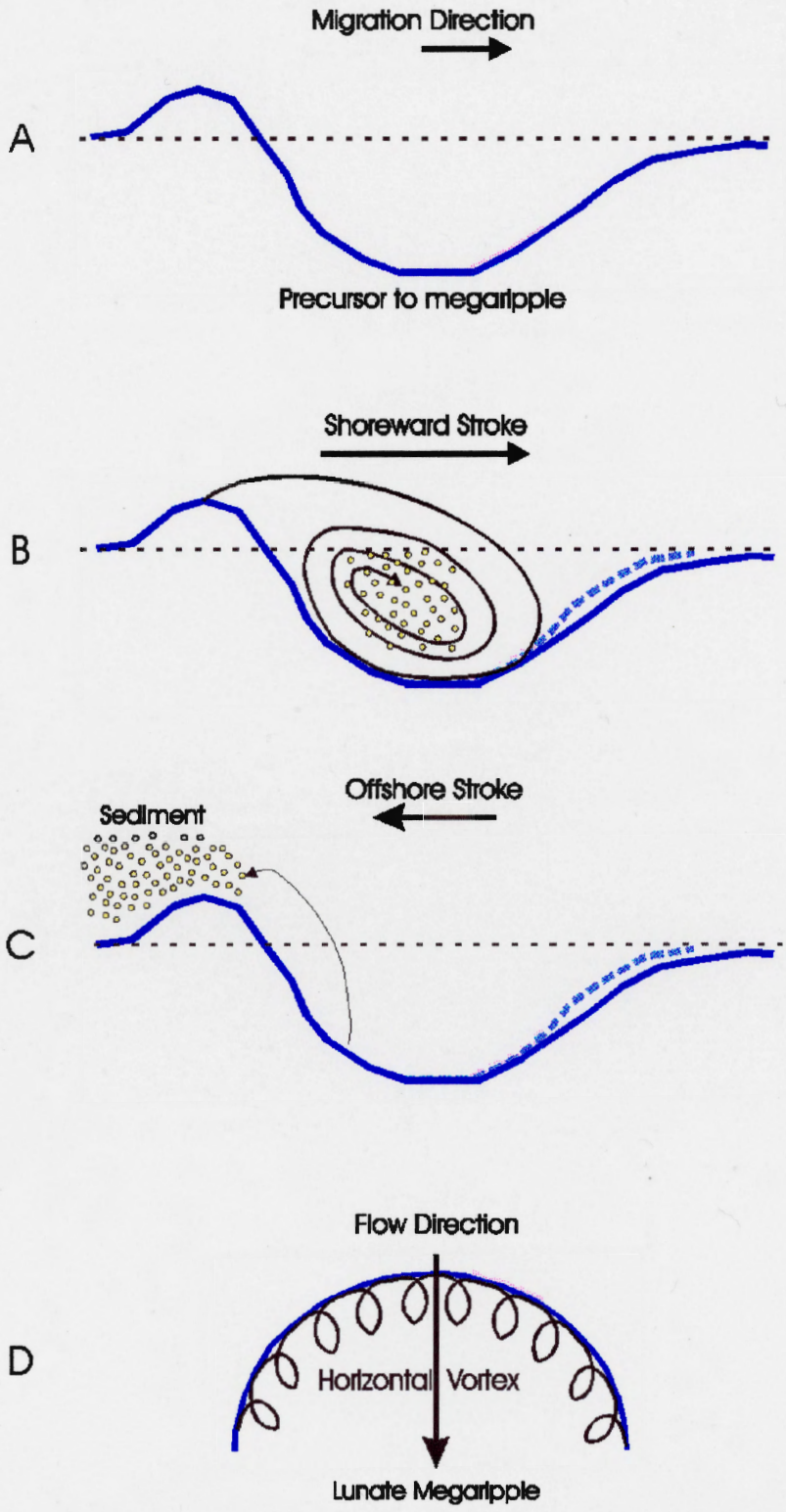

Figure 4.11 Schematic diagram of the formation of horizontal vortex in a lunate megaripple. Dashed blue lines are the bed profiles before the shoreward stroke and solid blue lines are the bed profiles after the shoreward stroke.

Chapter 5: SUMMARY AND CONCLUSIONS

5.1 Summary

The goal of this thesis was to examine the SandyDuck97 data to identify pock mark occurrence, their geometric characteristics, and migration patterns in order to determine the relationship between pock mark formation and hydrodynamic conditions. Pock marks are shown to have occurred during all 13 storm events and specifically during the growth and decay of 12 of these storms. The quantitative analysis concentrates on 189 fan beam images of pock marks between yeardays 264 and 275 representing a total of 1000 pock mark subimages. The mean physical characteristics of these features are summarized in Table 5.1.

Shape	Circular
Diameter	17cm
Area	270cm^2
Depth	~3cm
Nucleus	
In subimages	112/1000
In distinct PM	12/138
Number Density	5/80m^2
Group Lifetime	4.5h

Table 5.1 Mean characteristics of pock marks during SandyDuck97 where PM= pock marks.

Of the forcing conditions acting in the nearshore environment during SandyDuck97, the wave orbital velocity appears to have been the primary forcing parameter controlling the occurrence of pock marks. Pock marks occurred in a range of wave orbital velocities of 50cm/s-115cm/s during which time they sometimes appeared

simultaneously with linear ripples and lunate megaripples. At the upper wave orbital velocity, the seafloor becomes a flat bed and no bedforms, including pock marks, appear.

On average, pock marks are approximately circular depressions, 10-30cm in diameter and 3cm in depth. Although the mean diameter of these features is 17cm, they can be as small as 4cm and as large as 75cm. There is a tendency for pock marks to be larger during storm growth than during storm decay. It is possible that there is a bias towards the deepest part of the depression in those diameters determined using the edge detection algorithm. This can result in diameters as much as 2 times smaller than those determined using the pencil beam data.

The number density of pock marks that occur in the $80m^2$ field of view of the fan beam image varies widely from 1 to 22. Some pock marks appear and disappear in the fan beam image fairly quickly (in as little as 20min) which in some cases give the image a twinkling or blinking appearance. Other pock marks have a longer lifetime and their migration direction can be followed in the sonar images. There is a tendency for more pock marks to occur during the growth of a storm than during decay.

The data partially support the theory that pock marks form due to scour about a nucleus (possibly a shell or pebble). Shells and pebbles of necessary sizes were seen on the beach at the end of the storm events. Of the 189 fan beam images analyzed, 112 out of 1000 pock mark subimages contained a nucleus representing 12 of 138 distinct pock marks. This 10% nucleus occurrence frequency may be an underestimate, as the nuclei may be too small or too deep within the pock mark depression for the fan beam sonar to detect.

It is also possible that there are other pock mark formation mechanisms. The large pockmarks seen on the Scotian shelf and in the North Sea are degassing or dewatering features. The small pock marks which appeared at SandyDuck97 may be a smaller version of such an occurrence. This theory is improbable however as pock marks are so closely related to wave orbital velocity. Another method of formation may be from a number of possible vortex generation mechanisms. One such mechanism may be due to tornado vortices that break off from the horizontal vortices that occur as a wave breaks. These eddies may touch the seafloor causing sand particles to be suspended and washed away, leaving behind a depression. If pock marks only formed during storm growth it is unlikely there would be evidence of them in the rock record as they disappear at the peak of storms. Since they do occur during storm decay, however, it is possible that under certain conditions, pock marks may be preserved in the geological record.

The importance of these pock marks is their possible role as a precursor to lunate megaripple genesis. These large bedforms contribute significantly to bottom roughness at high wave energy and are therefore important in the prediction of sediment transport. Only six pock marks developed into lunate megaripples as they migrated during the 75-day experiment and this only occurred during storm growth. The hydrodynamics related to this development varied and no definite circumstances for the transformation could be determined.

5.2 Conclusions, Recommendations, and Future Work

Although the physical characteristics of pock marks have been determined using fan beam and pencil beam data, some other relevant characteristics such as migration

rates and growth and decay patterns and rates have yet to be analyzed. More work is needed in these areas to better understand the relationship between pock marks and the nearshore hydrodynamics and establish a link between these features and sediment transport. At present, the hydrodynamics of pock mark formation can only be constrained between a wave orbital velocity of 50 to 115cm/s (with analyzed data further constrained to between 60-100cm/s). It is also unknown, as of yet, if pock marks form during the accretion or erosion of sediment. This could be quite useful in determining if these features can be preserved in the rock record.

It is apparent from the data that nuclei may play an important role in the formation of pock marks. Although the percentage of pock marks containing a nucleus was low, there are explanations for this concerning the detection limits of the instruments. It would be beneficial to pock mark understanding to perform laboratory tests in this area. Pock marks of varying sizes could be generated in a wave tank for nuclei of varying shapes, sizes, and sorts (i.e. flat shell and rounded pebbles). These would then be scanned using the fan beam sonar to see which nuclei can be detected and how often.

More research needs to be done on the development of pock marks into lunate megaripples. There were only six cases of this event in the data set, which does not give conclusive evidence as to what conditions are required for this process to occur.

Given their frequency of occurrence during SandyDuck97 and their occasional development into lunate megaripples, the absence of any previous work on these features in the published literature is surprising and raises many questions. Have these features really never been seen before? Is it possible that pock marks were not previously

observed because of the limitations of other bedform measurement equipment? Is it possible that pock marks have gone unrecognized in the geological record? Is a nucleus required for pock mark formation and do lunate megaripples always form from pock marks? Despite all the remaining questions an important result of this thesis project has been to demonstrate that during SandyDuck97 pock marks did occur during every storm event, and for all events but one, pock marks occurred during both storm growth and decay.

APPENDIX A: LOCATION OF POCK MARKS

Isum	Subimages
_007	A-U
_008	B,D,E,G-J,N,P,Q,U
_009	D,E,I,J,L,Q,U
Total isums = 4 Total different images = 21	

Table A-1 Number of different pock mark images between 264.05-264.07.

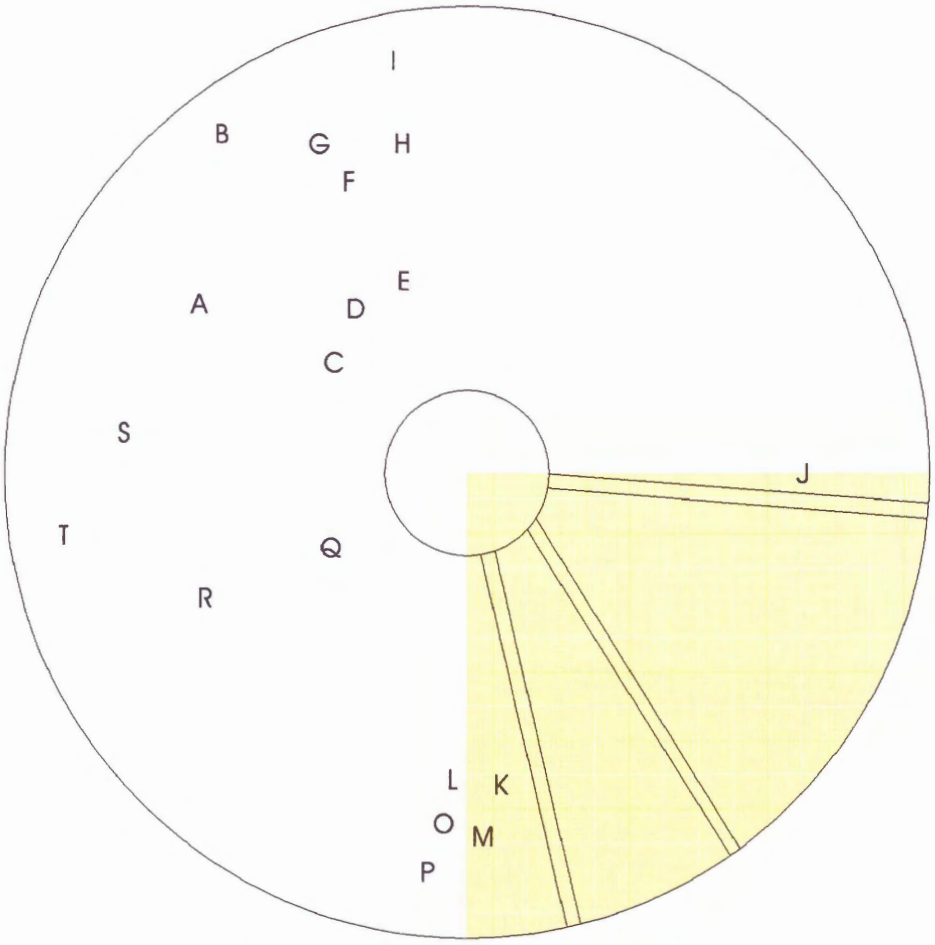

Figure A-1 Diagram of the pock mark locations at time 264.05-264.07. Yellow shading represents the area around the instrument frame that may effect pock mark formation.

Isum	Subimages
_088	A,B
_089	**A**,B,C
_090	**A**,B-D
_091	**A**,B
_092	**A**,B
_093	**A**
_094	**A**
_095	**A**
Total isums = 8	
Total different images = 4	

Table A-2 Number of different pock mark images between 264.69-264.73. Bold letters indicate the pock mark contains a nucleus.

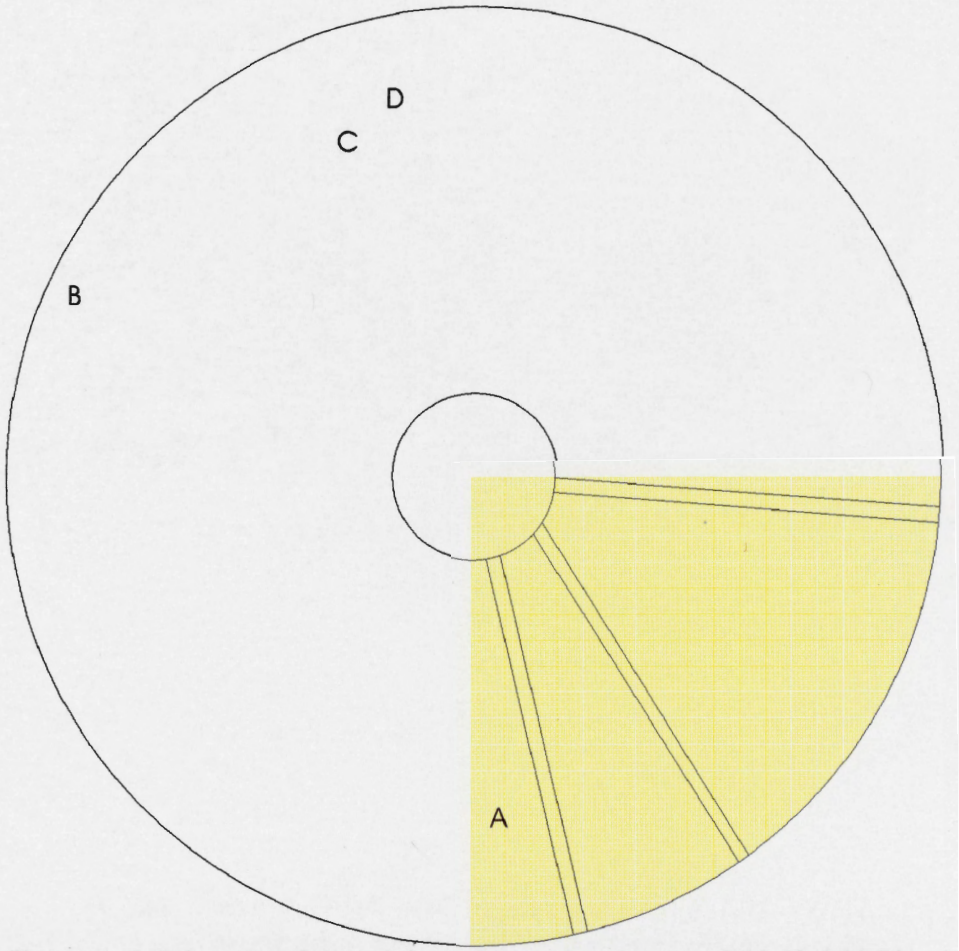

Figure A-2 Diagram of the pock mark locations at time 264.69-264.73. Yellow shading represents the area around the instrument frame that may effect pock mark formation.

Isum	Subimages	Isum	Subimages
_004	A,B	_010	C,D,I,L,M
_005	A-E	_011	C,D,I,L,M
_006	A-I	_012	C,D,I
_007	B-K	_013	C,**D**,I
_008	C,D,I,J	_014	C,**D**,I
_009	C,D,I,J	_015	I
Total isums = 12 Total different images = 18			

Table A-3 Number of different pock mark images between 267.08-267.27. Bold letters indicate the pock mark contains a nucleus and underlined letters are pock marks that transform into lunate megaripples.

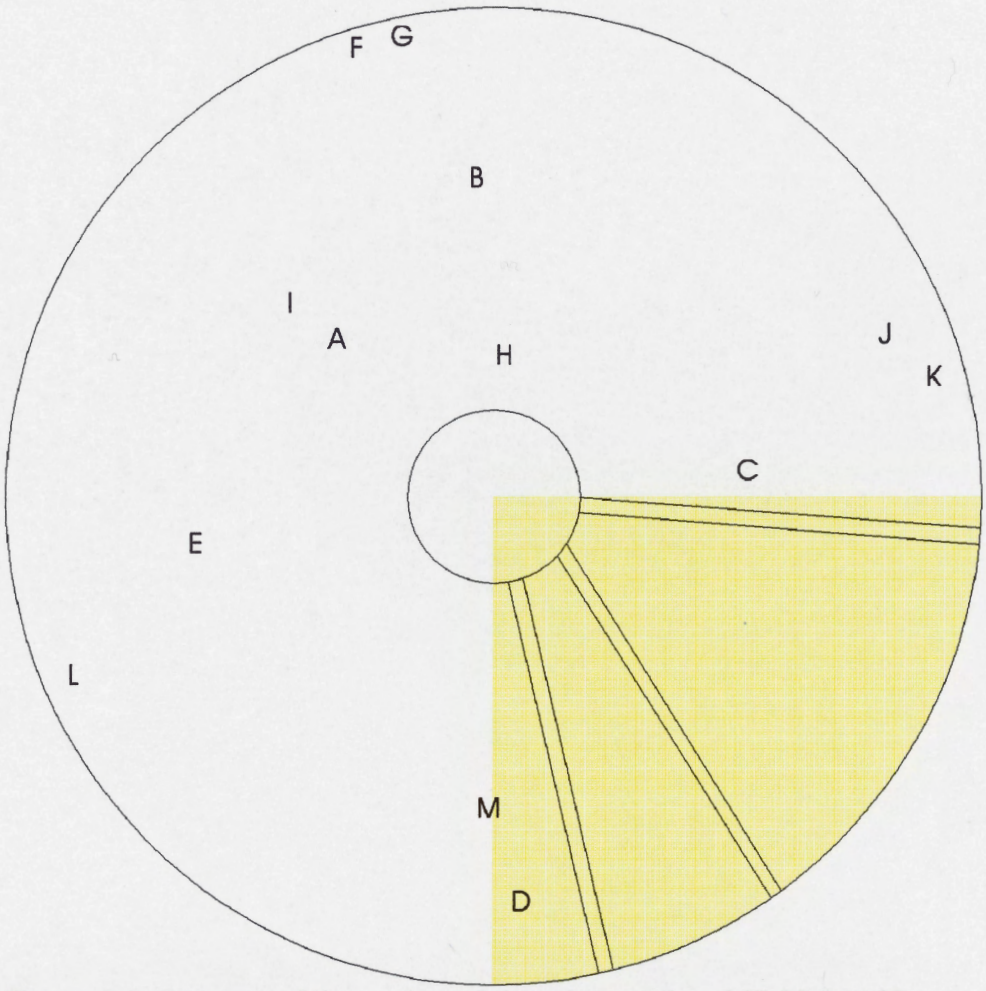

Figure A-3 Diagram of the pock mark locations at time 267.08-267.27. Yellow shading represents the area around the instrument frame that may effect pock mark formation.

Isum	Subimages	Isum	Subimages
_055	A,**B**,C	083	**B**,\,^
_056	A,**B**,C,D	084	**B**, ,^
_057	A,**B**,C,E	085	**B**, ,`,a
_058	A,**B**,C,E	086	**B**,^, ,`,a
_059	A,**B**,C,E	087	**B**,^, ,`
_060	A,**B**,C,F	088	**B**, ,`,b
_061	A,**B**,C,F	089	**B**, ,`,b,c
_062	A,**B**,F,G	090	B, ,`,b,c,d
_063	A,**B**,F,G	091	B, ,`,b,d,e
_064	A,**B**,F	092	B, ,`,b,d-f
_065	A,**B**,F,H	093	B, ,`,b,d-f
_066	A,**B**,H-J	094	**B**,`,e,g-i
_067	A,**B**,H,J-M	095	B,`,e,g-j
_068	**B**,H,J-R	096	B,`,e,i-k
_069	**B**,H,K-M,O-R	097	**B**,`,e,i,k
_070	**B**,H,K-M,O,P,R-T	098	**B**,`,e,k
_071	B,H,K-M,O,Q-T	099	**B**,`,e,i,k
_072	B,L,M,O,R-U	_100	**B**,`,e,i,k
_073	B,L,M,O,U	_000	**B**,`,i,k,l
_074	**B**,L,M,O,U	002	B,`,i,l
_075	**B**,L,O,U,V,**W**,X	003	**B**,`,i
_076	**B**,L,O,U,V-Y	004	**B**,`,i
_077	**B**,L,U,W-Y	005	**B**
_078	**B**,U,**W**	006	**B**,m,n
_079	**B**,U	007	B,m,n
_080	B,Z,[,\,]	_008	**B**,n
_081	B,Z,[,\,],^	_009	B
082	**B**,Z,[,\,^		
Total isums = 57 Total different images = 52			

Table A-4 Number of different pock mark images between 267.69-268.06. Bold letters indicate the pock mark contains a nucleus.

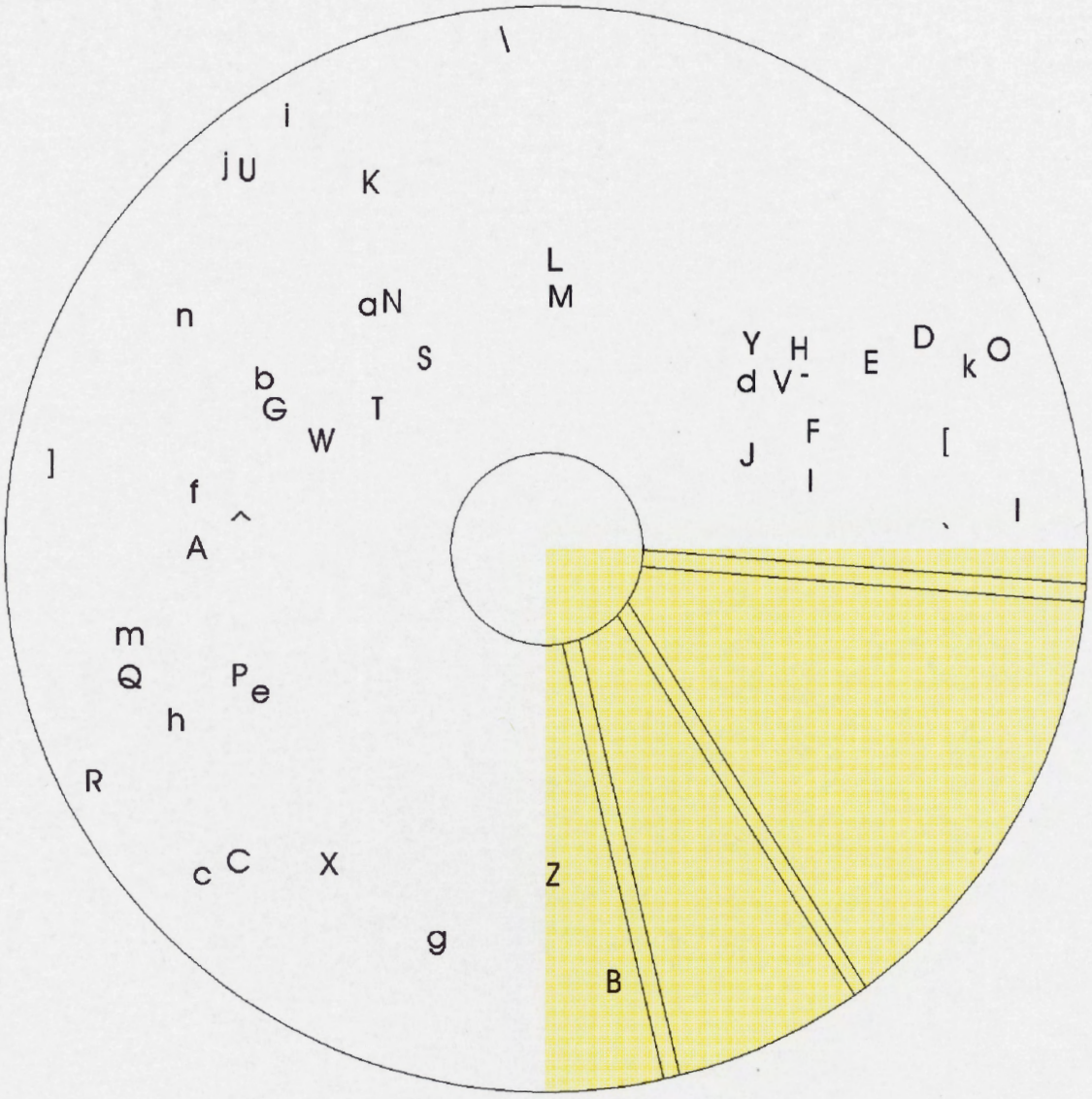

Figure A-4 Diagram of the pock mark locations at time 267.69-268.06. Yellow shading represents the area around the instrument frame that may effect pock mark formation.

Isum	Subimage	Isum	Subimage
_019	A,B,C,**D**	044	**D**,F,H-K
_020	A,B,C,**D**	045	F,H-K
_021	A,C,E	_046	F,H-K
_022	C-G,**D**	047	F,H-K
_023	**D**-G	048	F,H,I,K
_024	**D**,F,G	049	F,H,K,N-P
_025	**D**,F H	050	F,H,K,N-Q
_026	**D**,F H	051	F,H,I,K,**N**,O,Q
_027	**D**,F H	052	F,H,I,K,**N**,O,Q
_028	**D**,F H	053	F,H,I,K,**N**,O,Q,**R**-T
_029	F,H,I	_054	H,I,K,**N**,O,Q,**R**,T-Y
_030	F,H,I	_055	H,I,K,**N**,O,Q,R-[
_031	F,H,I	_056	H,I,K,**N**,O,R-^
_032	D,F,H-K	_057	H,I,K,**N**,R-'
_033	**D**,F,H-K	058	H,I,K,N,R-a
_034	**D**,F,H-K	059	H,I,K,N,R-a
_035	D,F,H-K	060	H,K,N,R-b
_036	D,F,H-K	_061	H,K,N,R-Z,\-c
_037	D,F,H-L	_062	H,K,N,R-Z,\-^,b,c
_038	D,F,H-M	_063	H,K,N,S-Z,\-^,',b
_039	D,F,H-M	_064	H,K,T,W-X,\-^,'
_040	D,F,H-K	_065	H,K,T,W,],'
_041	**D**,F,H-K	066	K,W
_042	**D**,F,H-K	067	K,W
_043	**D**,F,H-K		
Total isums =49 Total different images = 34			

Table A-5 Number of different pock mark images between 270.39-270.86. Bold letters indicate the pock mark contains a nucleus.

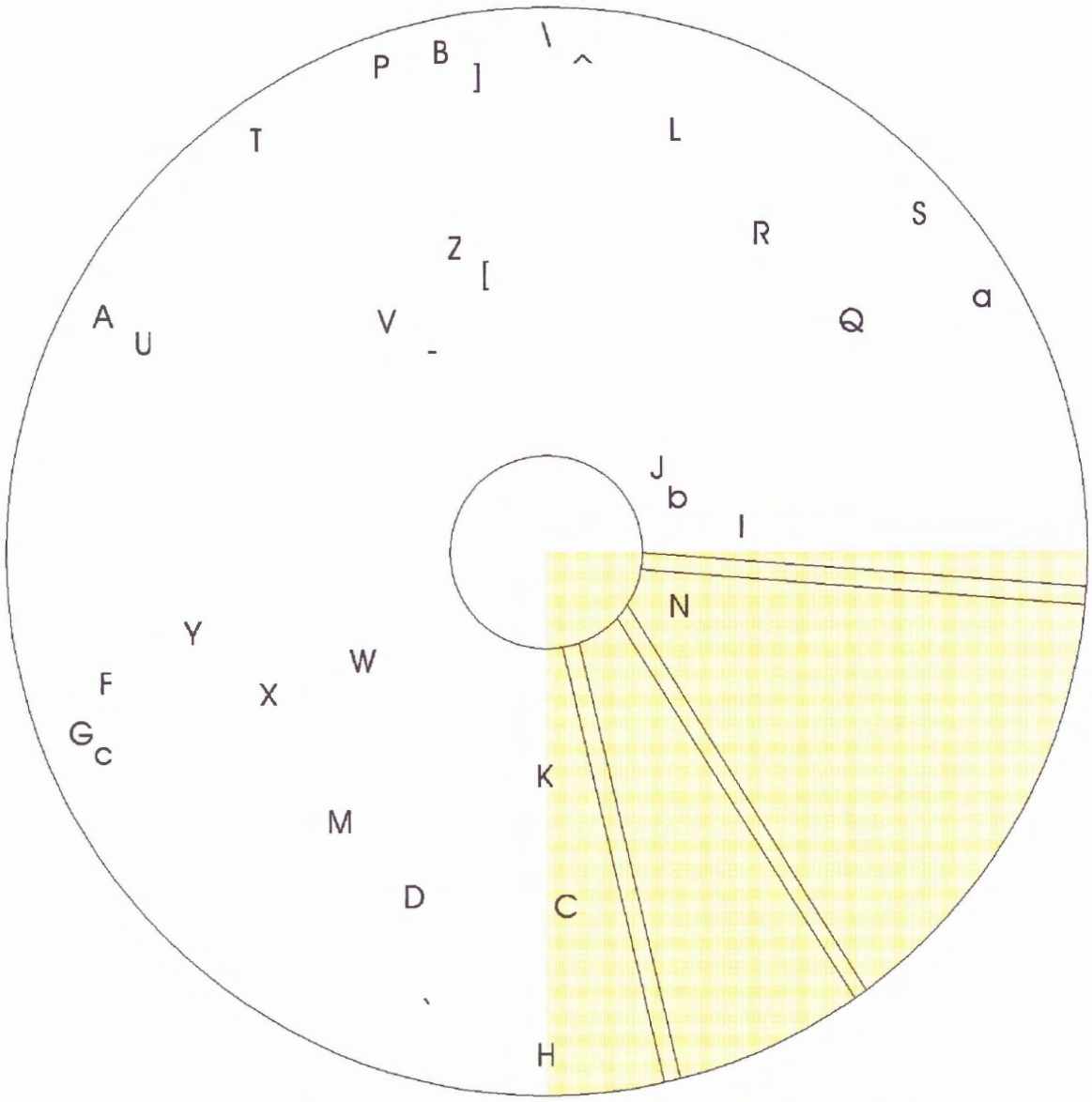

Figure A-5 Diagram of the pock mark locations at time 270.39-270.86. Yellow shading represents the area around the instrument frame that may effect pock mark formation.

Isum	Subimages	Isum	Subimage
_090	A-C	_110	C,Q,H
_091	B,**C**	_111	**C**,H,L,M,N,Q
_092	B,**C**,D	_112	C,H,L,M,N,Q
_093	**C**	_113	C,**F**
_094	C,E,F	_114	C,**F**,H
_095	**C**	_115	C,**F**,H
_096	**C**	_116	C,**F**,H,R
_097	**C**	_117	C,**F**,H,R
_098	**C**	_118	C,H,R,S
_099	**C**	_119	C,F,H,N,R,S
_100	**C**	_120	C,F,H,L-N,R,T
_101	**C,F**	_121	C,F,G,H,L,N
_102	**C**,F-H	_122	C,F,G,H
_103	**C**,F-I	_123	C,F,G,H,N,U
_104	C,F,H,I	_124	C,F,H,U
_105	C,F-O	_125	C,F,G,H,M,N,O
_106	C,**F**,G,H,J-Q	_126	C,F,G,H,N,U
_107	**C**,**F**,G,H,L,M,P,Q	_127	F,H
_108	**C**,H,L,M,Q	_128	H
_109	**C**,M,Q	_129	H
Total isums = 41 Total different images = 21			

Table A-6 Number of different pock mark images between 271.67-271.99. Bold letters indicate the pock mark contains a nucleus.

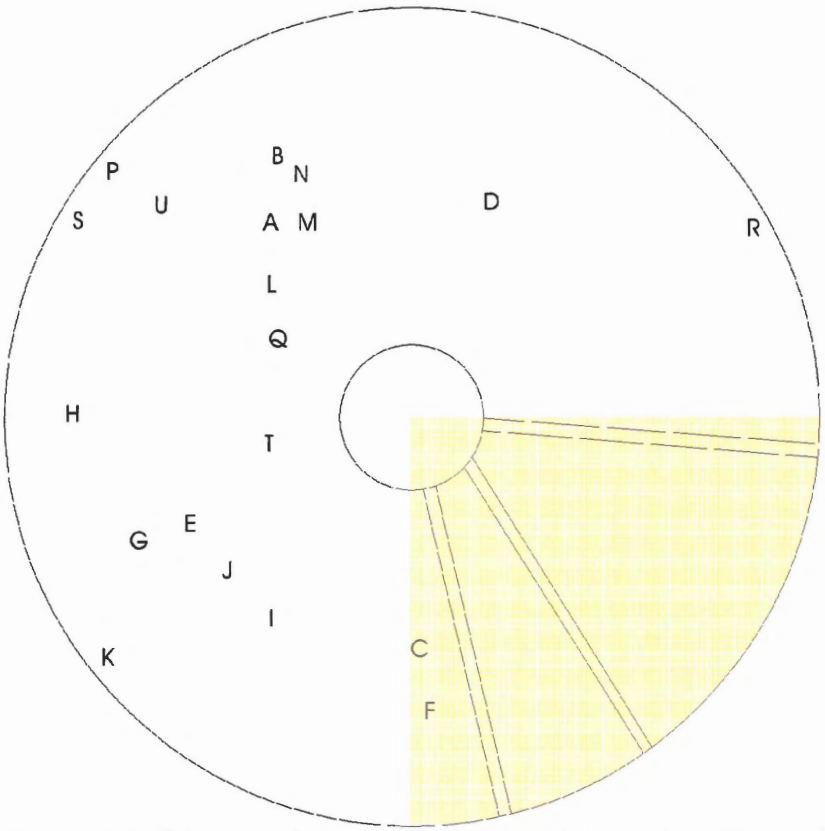

Figure A-6 Diagram of the pock mark locations at time 271.67-271.99. Yellow shading represents the area around the instrument frame that may effect pock mark formation.

Isum	Subimages
_075	A-C
_076	A-F
_077	A-G
_078	B-J
_079	C-G,J,K
_000	E,G,J,K
_001	E,G,J-M
_002	K-N
_003	K,N
Total isums = 9	
Total different images = 19	

Table A-7 Number of different pock mark images between 274.96-275.00.

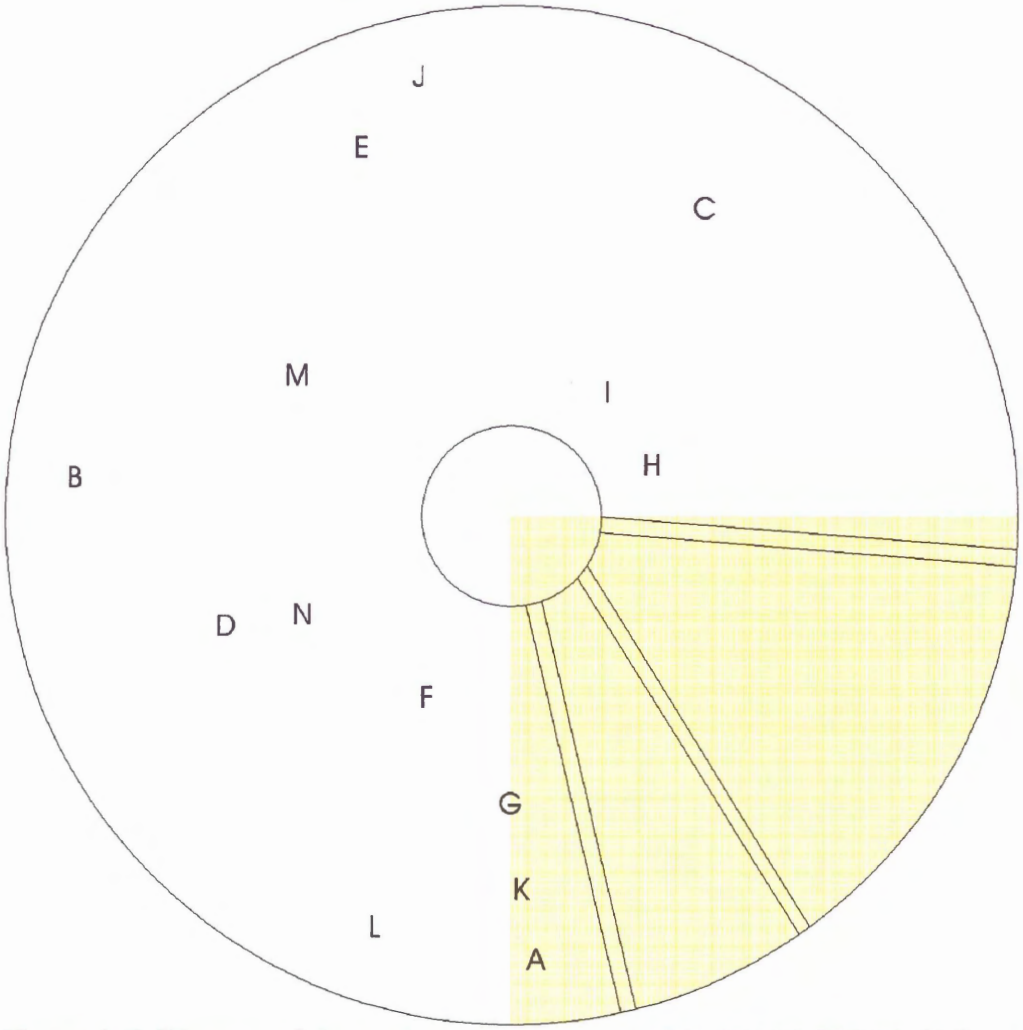

Figure A-7 Diagram of the pock mark locations at time 274.96-275.00. Yellow shading represents the area around the instrument frame that may effect pock mark formation.

Isum	Subimages	Isum	Subimages
_049	A,B	_056	A,B
_050	A,B	_057	A,B,F
_051	A,B	_058	A,B,F
_052	A-E	_059	A,B,F
_053	A-E	_060	A,B
_054	A,B,E	_061	A
_055	A,B,E		
Total isums = 13			
Total different images = 13			

Table A-8 Number of different pock mark images between 275.34-275.47.

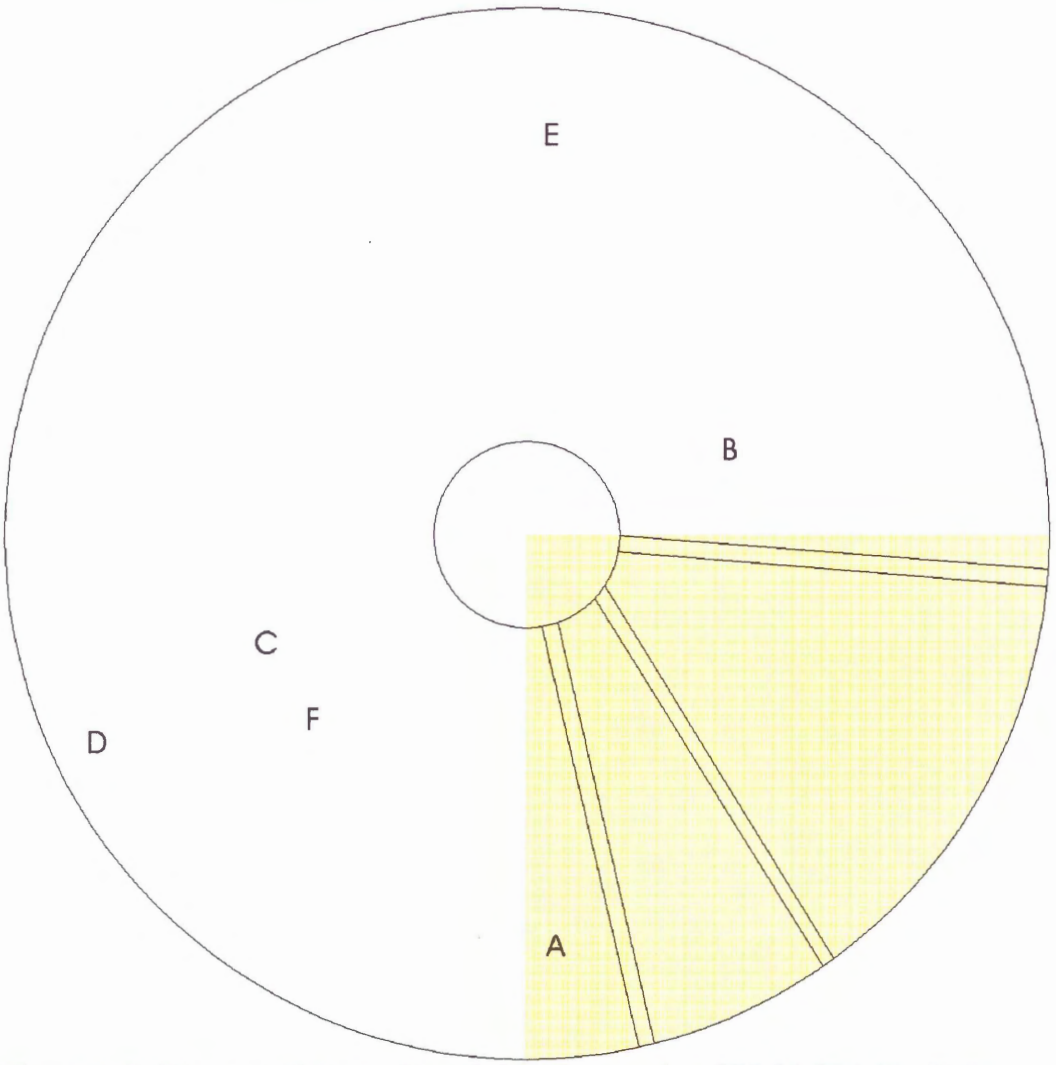

Figure A-8 Diagram of the pock mark locations at time 275.34-275.47. Yellow shaded portion represents the area around the instrument legs which was ignored.

Time	Pock Marks in Shaded Area
264.05-264.07	J,K,M
264.69-264.73	A
267.08-267.27	D,M
267.69-268.06	B,Z
270.39-270.86	C,H,K,N
271.67-271.99	C,F
274.96-275.00	A,G,K
275.34-275.47	A

Table A-9 Pock marks that may be affected by the legs of the instrument frame.

APPENDIX B: DESCRIPTION OF DATA SET

Frame	Time					
.fli	Start	Stop	Start	Stop	Number	Comments
FanC_237-240	237 19:15	238 7:22	_027	_044	3--8	Popcorn, Migrating, forms LM
	238 19:33	239 3:52	_091	_023	1--3	Small, LM in frame
	240 0:57	240 1:37	_005	_009	1	V.small, LM in frame
						NOTE:no velocity data for 237-238.5
FanC_241-244						LM
FanC_245-248	246 20:02	246 21:02	_000	_006	6	Form LM
	247 23:12	248 1:42	_129	_010	1--4	Small, Migrating
	248 2:42	248 5:02	_016	_030	2	Small, Popcorn
	248 7:12	248 16:42	_039	_066	1--4	Small, Migrating, Popcorn
						NOTE:no velocity data for 246.7-246.8 and no movie for 245 6:52 - 246 20:02
FanC_249-252	251 9:32	251 20:32	_019	_051	1	PM -> LM
	252 15:06	252 16:32	_010	_013	2--8	Very fast
						NOTE:no velocity data for 252.2-253
FanC_253-256	253 0:02	253 5:32	_000	_011	2	Small
	253 19:42	254 0:52	_056	_005	2--8	Popcorn, Migrating
	254 5:12	254 11:32	_031	_069	2	Migrating, Fairly large
	254 16:32	254 18:22	_097	_108	4--6	Popcorn, Migrating
	256 3:42	256 4:12	_022	_025	2	Small
	256 18:32	256 23:32	_057	_067	2--4	Small, Popcorn
						NOTE:no velocity data for 253-253 19:52
FanC_257-260	258 10:22	258 12:32	_021	_025	1	Large, Migrating
	259 3:02	259 5:32	_006	_010	6	Small
						NOTE:no velocity data for 259 5:02 - 259 16:02 and 260 1:01 - 260 14:02
FanC_261-264	264 1:12	264 1:42	_007	_010	>30	Migrating, Forms LM
	264 15:42	264 17:12	_088	_095	3--4	Migrating
	264 18:32	264 18:52	_103	_105	1	
	264 21:42	264 23:32	_122	_132	5	
						Note:no velocity data for 263 9:02-263 12:02
FanC_265-268	265 0:12	265 10:02	_001	_059	1--10	Popcorn, Migrating
	265 19:52	265 21:20	_118	_125	1--6	Popcorn, Small
	267 2:02	267 6:02	_004	_012	11	Migrating, 1 PM -> LM
	267 12:32	267 13:02	_032	_035	1	Migrating
	267 16:32	268 1:32	_055	_009	15	Popcorn, Small
	268 6:32	268 10:12	_039	_061	3	Large
FanC_269-272	270 9:32	270 20:32	_019	_067	>20	Only 2 PM from 019-053
	271 16:02	272 0:02	_090	_000	10	Migrating

Frame	Time					
.fli	Start	Stop	Start	Stop	Number	Comments
FanC_273-276	274 23:12	275 0:32	_075	_003	12	Migrating
	275 8:12	275 11:12	_049	_061	4	1 Migrating
FanC_277-283	279 17:32	279 21:32	_126	_042	2	Migrating
FanC_281-284	282 1:32	282 5:02	_003	_010	2	
	282 22:02	282 23:32	_044	_047	1	Migrating
	284 6:32	284 8:42	_039	_052	1	Migrating
	284 18:32	284 21:02	_099	_103	5	Popcorn
FanC_285-288	287 1:32	287 2:32	_003	_005	1	Formed large bedforms
	288 9:02	288 10:52	_038	_049	1	Migrating
	288 11:42	288 13:52	_054	_067	2	Migrating
	288 17:32	288 22:32	_079	_109	6	Popcorn, Migrating
FanC_289-292	290 19:22	290 23:32	_103	_126	6	Popcorn
FanC_293-296	295 15:42	295 17:12	_082	_091	2	Migrating
	296 0:32	296 2:42	_003	_016	5	Popcorn
						NOTE:no velocity data from 296 16:02-23:02
FanC_297-300	298 2:32	298 6:32	_005	_013	3	Popcorn
	298 22:32	300 4:12	_042	_025	13	Popcorn, Migrating
	300 21:12	300 23:12	_098	_102	12	
FanC_301-304	301 1:02	301 2:32	_006	_015	2--3	Migrating
	301 23:42	302 0:32	_126	_003	2	
	304 17:12	304 23:52	_053	_093	6	LM at start
FanC_305-308	305 0:02	305 0:052	_000	_005	6	
	305 16:22	306 18:42	_092	_105	15	Lots of small, Popcorn
FanC_309-312	309 0:02	310 6:22	_000	_038	>15	Lots of small popcorn, Few big migrating
	312 12:22	312 16:32	_066	_081	7	Small, Popcorn
	312 22:32	312 23:52	_110	_118	8	Small, Popcorn
FanC_313-315	313 1:22	313 2:02	_005	_009	6	
	313 7:02	303 8:02	_039	_045	3	
FanD_237-240	237 14:08	237 22:12	_000	_041	7	Large, Migrating
	238 0:12	238 2:22	_001	_014	7	Large, Migrating } all form at same spot
	238 12:12	238 13:12	_058	_064	1	Large, Migrating
	239 3:02	239 4:22	_018	_026	1	Migrating
	239 16:52	239 19:32	_089	_105	3	Large, Migrating, LM at end
						NOTE:no velocity data from 237-238 13:22
FanD_241-244						3 LM

Frame	Time					
.fli	Start	Stop	Start	Stop	Number	Comments
FanD_245-248	248 8:02	248 8:32	_044	_047	1	Migrating
	248 16:32	248 18:22	_087	_098	4	Small
						NOTE:no velocity data from 245-246.75
						NOTE:no movie from 245 6:42-246 20:02
FanD_249-252	250 9:32	250 11:32	_019	_023	1	Large, Near centre, Migrating
						NOTE:no velocity data from 252.5-253
FanD_253-256	254 2:12	254 4:12	_013	_025	4	2 LM
						NOTE:no velocity data from 253-253 19:52
FanD_257-260	257 2:02	257 5:32	_004	_011	4	Small, Popcorn
						NOTE:no velocity data from 260 1:31-16:20
						NOTE:no data from 259 5:02-259 16:02
FanD_261-264	264 19:42	264 20:42	_110	_116	1	Stationary
						NOTE:no velocity data from 263 8:32-12:32
FanD_265-268	265 3:52	265 5:52	_022	_034	3	
	267 16:22	267 22:42	_055	_093	4	Popcorn
	268 6:22	268 9:22	_038	_056	5	Migrating
						NOTE:no velocity data from 268 17:12-20:52
FanD_269-272	270 18:52	270 20:02	_057	_064	3	Stationary
	271 22:02	271 23:32	_126	_129	1	Migrating
FanD_273-276						
FanD_277-276						
FanD_281-284	283 0:32	283 2:02	_001	_004	1	Small, Migrating
	284 17:52	284 18:22	_095	_098	1	Small, Migrating
FanD_285-288	285 7:02	285 9:59	_014	_018	1	Migrating
	285 21:32	286 1:32	_037	_003	2	Migrating
	288 9:02	288 10:12	_039	_045	3	Migrating
FanD_289-292						
FanD_293-296	295 16:32	295 17:02	_087	_090	1	Stationary, Small
	295 20:42	295 22:42	_112	_124	3	Stationary, Small
						NOTE:no velocity data from 295 8:42-10:22
FanD_297-300	298 20:32	299 8:12	_041	_049	15	Popcorn, Migrating
	300 4:12	300 6:12	_025	_037	3	
	300 21:32	300 23:02	_098	_101	8	1 forms a LM, Small, Migating

Frame	Time					
.fli	Start	Stop	Start	Stop	Number	Comments
FanD_301-304	301 5:02	301 6:02	_030	_036	4	Small, Migrating
	304 21:02	304 23:52	_076	_093	10	Small, Migrating, Popcorn
FanD_305-308	305 19:15	305 20:32	_107	_115	1	Stationary
FanD_309-312	309 5:02	309 5:52	_030	_035	1	Migrating } Start at same place
	309 20:12	309 21:52	_118	_125	1	Migrating }
FanD_313-314	313 4:22	313 5:32	_023	_030	2	Stationary
	313 7:32	313 8:22	_042	_047	4	Stationary
FanF_259-260	259 20:32	259 21:32	_021	_023	1	Migrating
FanF_282-284	284 3:42	284 4:02	_022	_024	1	Very Small
	284 4:42	284 5:12	_028	_031	1	Migrating
FanF_285-288	287 4:02	287 7:02	_008	_014	2	Migrating
	288 5:42	288 9:02	_026	_038	5	
Mean					4.5	

REFERENCES

Allen, J.R.L. 1982a. Sedimentary Structures: Their Character and Physical Basis. Elsevier, Amsterdam, 1, 593 p.

Allen, J.R.L. 1982b. Sedimentary Structures: Their Character and Physical Basis. Elsevier, Amsterdam, 2, 663 p.

Bagnold, R.A. 1946. Motion of waves in shallow water. Interaction between waves and sand bottoms. Proc. R. Soc. London, Ser. A, 187, pp. 1-16.

Birkemeier, W.A., Miller, H.C., Wilhelm, S.D., DeWall, A.E., and Gorbics, C.S. 1985. A User's Guide to the Coastal Engineering Research Center's (CERC's) Field Research Facility, Institution Report CERC-85-1, Department of the Army, US Army Corps of Engineers, Washington, DC., 137 pp.

Clifton, H.E. 1976. Wave-formed sedimentary structures – A conceptual model. In: R.A. Davis, Jr. and R.L Ethington (Editors), Beach and Nearshore Sedimentation. SEMP Spec. Publ., 24, pp. 126-148.

Clifton, H.E. and Dingler, J.R. 1984. Wave-formed structures and paleoenvironmental reconstruction. Mar. Geol., 60, pp. 165-198.

Dingler, J.R., Hunter, R.E., and Phillips, R.L. 1971. Depositional structures and processes in the non-barred high-energy nearshore. J. Sediment. Petrol., 41, pp. 651-670.

Dingler, J.R., and Clifton, H.E. 1984. Tidal cycle changes in oscillation ripples on the inner part of an estuarine sand flat. Mar. Geol., 60, pp. 219-233.

Eadie, R.W. and Herbich, J.B. 1986. Scour about a single, cylindrical pile due to combined random waves and current. Coastal Engineering, V 3, pp. 1858-1870.

Field, M.E. and Duane, D.B. 1976. Post-Pleistocene history of the United States Inner Continental Shelf: Significance of origin of Barrier Islands. Geol. Soc. Am. Bull., 87, pp. 691-702.

Hay, A.E. 2000. Personal communication. Dalhousie University.

Hay, A.E. and Bowen, A.J. 1993. Spatially correlated depth changes in the nearshore zone during autumn storms. J. Geophys. Res., 98(C7), pp. 12,387-12,404.

Hay, A.E. and Bowen, A.J. 1999. Alongshore Migration of lunate megaripples during DUCK94: Part 1, Orthogonal waves and currents. J. Geophys. Res. 99 (In Press).

Hay, A.E. and Wilson, D.J. 1994. Rotary sidescan images of nearshore bedform evolution during a storm. Mar. Geol., 119, pp. 57-65.

Hovland, M. 1982. Pockmarks and the Recent Geology of the Central Section of the Norwegian Trench. Mar. Geol., 47, pp. 283-301.

Hovland, M. and Judd, A.G. 1988. Seabed Pockmarks and Seepages-Impact on Geology, Biology and the Marine Environment. Graham & Trotman, London, 293 p.

Hoyt, J.H. 1967. Barrier Island Formation. Geol. Soc. Am. Bull., 78, pp. 1125-1136.

Hunter, R.E., Clifton, H.E. and Philips, R.L. 1979. Depositional processes, sedimentary structures, and predicted vertical sequences in barred nearshore systems, Southern Oregon Coast. J. Sediment. Petrol., 49, pp. 711-726.

Kamar, P.D. 1976. Beach Processes and Sedimentation. Prentice-Hall, Englewood Cliffs, N.J., 417 p.

King, L.H. and MacLean, B. 1970. Pockmarks on the Scotian Shelf. Geol. Soc. Am. Bull., 81, pp. 3141-3148.

Nielsen, P. 1981. Dynamics and geometry of wave-generated ripples. J. Geophys. Res., 86, pp. 6467-6472.

Nielsen, P. 1992. Coastal Bottom Boundary Layers and Sediment Transport. World Scientific, River Edge, NJ, 324 p.

Sleath, J.F.A. 1984. Sea Bed Mechanics, John Wiley & Sons, New York, 335 p.

Schwartz, R.K., Cooper, D.W., and Etheridge, P.H. 1997. Sedimentologic Architecture of the Shoreface Prism, Relationship to Profile Dynamics, and Relevance to Engineering Concerns: Duck, North Carolina, Technical Report CHL-97-April 1997, U.S Army Engineers Waterways Experiment Station, Vicksburg, MS.

Vincent, C.E., and Osborne, P.D. 1993. Bedform dimensions and migration rates under shoaling and breaking waves. Cont. Shelf. Res., 13, (11), pp. 1267-1280.

www.frf.usace.army.mil/SandyDuck/SandyDuck.html. (1997).